Observations on the 1 xmg-1'cried Variability of the Gulf Stream Downstream of Cape Hatteras

Jorge Vazquez
Jet Propulsion Laboratory
California Institute of Technology
4800 oak Grow Dr. M/S 300-323
Pasadena, California 91109

email: jv@pacific.jpl.nasa.gov
phone: 818-3 s4-41s9

Short title: On the ljong-l'cried Variability of the Gulf Stream

ABSTRACT

To examine the long-period variability of the Gulf Stream sea level residuals relative to a two-year man sca level in the Gulf Stream downstream of Cape Hatteras (between 75°W and 60°W longitude) are used. Residuals, as (ic.rived from Geosat altimetry between 11/86 and 12/88, were gridded in space. and time at a temporal resolution of 10 days and spatial resolution of 1/4 degree. Complex empirical orthogonal function (CEOF) analysis was applied to the data set to extract the spatially correlated signal with the original data subsampled to 1/2 degree. in addition to determining the space-time scales and proj pagation characteristics of the different modes, wavenumber-frequency spectral techniques were used to separate the. variability into propagating and stationary components.

The CEOF technique applied to the. data set indicated that the first four CEOF modes accounted for 60% of the variability and were found to be above the. noise level 99% of the time.. CEOF 1 was associated with westward propagation at 5 km/day at a wave.icngdl of 2(WO km and eastward propagation at 1-2 km/day centered al a 500 km wavelength. This first CEOF is in good agree.nlc.nl with thin-jet equivalent barotropic models which predict westward propagation for wavelengths greater than 1130knl. A deflection of the wave.-likc. pattern at 65°W also indicates a possible topographic effect. A simple scaling of the effect of topography indicates that for length scales longer than the internal Rossby radius of deformation the topographic term is at least of the. same. order of magnitude as the Beta effect. The second CEOF was more broad-banded in wave.nu[llbcr space. with eastward propagation occurring in a wavenumber-frequency band between 300km-1400km and 0.5 c ycics/year -2.0 cycles/year. The third CEOF is similar in strac.lure. to the first, but with less energy. CEOF 4 was clearly identifiable with higher frequencies than the first three with westward propagation at 4 km/day. The spatial location of this mode. along with the westward propagation indicate.s possible influences from eddy/Stream interactions Thus topography, Rossby wave dynamics, and eddy/Stream interactions, all appear to have a significant role in determining the space.-tinm scales and propagation properties of the long-period response of sea level in the. Gulf Stream.

1. Introduction

The purpose of this paper will be to use sea level observations made by the Geosat altimeter in the region of the GulfStream downstream of Cape Hatteras (see Figure 1) and describe the mean and propagation properties of the long-period variability. Previous papers have shown that in this area satellite altimeter observations of sea level are useful in studying the Gulf Stream (Cheney, 1982; Fu et al., 1987; Kelley, K.A. and S.T. Gille, 1990; Vazquez et al., 1990; Zlotnicki, 1991). In the area downstream of Cape Hatteras the response of sea level at these long periods is influenced both by the meandering of the Stream and changes in Stream transport, Kelley and Gille (1990) showed that the annual cycle for the given area during the Geosat exact mission appears to have a maximum in the Fall and a minimum in the Spring. In addition to transport variations and the meandering of the Gulf Stream, eddy/Stream interactions should have an influence on sea level also. Recent models lend some insight into the response of sea level at the annual period and probable causes for the observed long-period response of sea level variations downstream of Cape Hatteras.

From nonlinear theory based on quasi-geostrophy, the response of sea level at the annual period should be in the form of baroclinic Rossby waves (Herrmann and Krauss, 1989) with a local concentration of energy in the area of the Gulf Stream as it leaves the coast off Cape Hatteras. Thus in the area of the Gulf Stream, long-period variability around the annual cycle should be influenced by the propagation of these Rossby Waves, the baroclinicity of the Gulf Stream appears to be important in determining the phase of the annual cycle since Greatbatch and Goulding (1989), using a linear wind driven barotropic model, were able to reproduce the phase of transport variations in the Florida Straits, but were unable to account for the annual cycle of transport in the Gulf Stream observed by Halkin and Rossby (1985) in the region downstream of Cape Hatteras. The exact nature of the annual cycle in surface transport of the Gulf Stream as it leaves the coast of Cape Hatteras is still a point of some controversy, with a recent paper by Kelley and Gille (1990) indicating a possible high in the Fall and a low in the Spring. Earlier papers by Fu et al. (1987), Worthington (1976), and Fuglister (1972) appear to indicate a maximum in transport in the late winter, early spring time frame and a minimum in early

fall, An annual cycle in the. Stream displacement, associated with the transport variability, is evident, as was pointed out by Tracey and Watts (1986). Thus, identification of the annual cycle in transport from sca level residual data alone is difficult since variations in Stream position c. ffect the sca level signature also. None.the.]css, in the. paper by Tracey and Watts (1 986), interannual variability was evident also, indicating a possible cause for the discrepancy in results. To clearly identify the mean annual cycle, a time series extending over several years is necessary. in this respect the Exact Re.peat Mission (ERM) of the. Geosat altimeter dots not provide. an ideal lime. series to study the annual cycle. of sea level variations, but nonetheless can provide, a unique opportunity for comparison of certain space-time properties of the lorlg-period response with previous observations and models.

Another possible. source of sea level variability at long periods in the give.rl area is due to eddy/Strcalll interactions. Ikeda (1981), using a twcj-layer quasi-geostrophic model, concluded that it was a combination of baroclinic instability, along with the beta affect, that was necessary for eddy formation. The view that baroclinic instability, arrd thus that potential energy, is the primary energy source for meander growth was challenged by Flierl et. al. (1987), but no conclusive evidence was shown for eddy detachment, although Rossby wave. radiation away from the barotropic jet was evident. An advantage of the Flierl mode.1 is the. inclusion of what is described as a pseudo-spectra while the Ikeda mode.1 is valid for only one frequency. ~'bus, the Flied model includes possible nonlinear effects due to energy cascades while, the, Ikeda model dots not. Mode.ting the, Gulf Stream using a piecewise uniform potential vorticity, Pratt and Stern (1986) were able to examine the d ynamics assoc. iated with eddy detachment for different meander amplitudes. In a later study Stern and Flierl (1987), using barotropic models, were able. to reproduce a westward propagation tendency as eddies, which were treated as point vorticities, interacted with the. front. Results will be compared with the. Stern and Flierl model, especially since westward phase, propagation is observed in an area of known eddy/Strcan~ interactions. in addition 10 these comparisons an equivalent barotropic thin-jet model (1-1/2 layer) dc.rived by Cushman-Roisin et al. (1992) predicts a critical wavelength where. the westward propagation tendency associated with Rossby waves is balanced by the. advection of the jet. A comparison will be made between the critical

wavelength predicted from this model and the propagation tendencies observed from the Geosat derived sea level wavenumber-frequency spectra

To identify the essential space.-timc. scale.s and propagation properties of the long-period response of sea level, complex empirical orthogonal function (CEOF) analysis was applied to the same data set used in Vazquez et al. (1990), where.by two years of the Geosat exact repeat mission (ERM) is used to construct an army of gridded sea level time series in an area bounded by 35°N to 43° N in latitude and 75°W to 60° W in longitude. The geographically correlated signal is then extracted via the CEOF analysis. Wavenumber-frequency spectral techniques are them applied to the. extracted geographically correlated signal to quantify the time-space scales and propagation properties of the. long-period variability in the region.

The data set used in this study was the. same as that used in Vazquez et al. (1990). For details on the processing of the. Geosat data as well as the creation of the spatially and temporally interpolated sea level residual maps see Zlotnicki et al. (1989(a,b)), Born et al. (1987) and Vazquez et al. (1990).

After initial processing of data from the Geosat exact repeat mission (Nov. 1986 - Dec. 1988) the data was interpolated to a regular grid in space and time using a successive correction scheme (Bratseth, 1986). The scheme is an iterative procedure whereby the interpolated values converge to the. data values after each successive. iterat ion. The weights involved include. a Gaussian function in the time domain and a Cressman function applied in the spatial domain. The c-folding time scale for the. Gaussian was chosen at five days and was based on a best fit scenario of interpolated values to the data. I Different spatial scales were used for each iteration, ranging from 1.2S degree for the first iteration to 0.5 degree for the last. 'Ibis formal smaller wale.s to converge for each successive iteration. The spatial window is chosen to include both points east and west of a given track (see Vazquez c1 al., 1990).

'ibis successive correction scheme, with the appropriate weights, was used to generate a data set of ten-day maps bet ween December], 1986 and November 30, 1988 al a 0.25° latitudinal and longitudinal resolution for the area between 35°N to 43° N and 75° W to 60° W (see Figure 1). Thus, a two- year time series of sea level residual (sea level with two-year mean removed at each grid point) was available at each grid point (x,y) with longitude "x" and latitude "y." These 74 maps formed the database for our CEOF and wavenumber- frequency anai ysis, whereby the CEOF anai ysis separated the data into uncorrelated mode.s of variability and the wavenumber-frequency analysis was applied to identify the spam-time scales and propagation properties of the.sc modes.

3. Complex EOF analysis

The technique of CEOF (Complex Empirical Orthogonal Function) analysis separates data into modes of variability whereby each of the modes is orthogonal and rri]corrc.late.d with other modes. Unlike real EOFs, where each mode represents a standing wave pattern, CEOFs can rc..solvc. propagating waves. For details on the. CEOF technique see Horel (1984) and Barnett (1983). In the Gulf Stream the decision to apply CEOFs instead of real EOFs is appropriate because of the wave propagation associated with the meandering of the Stream path. An alternative is to use real EOFs and combine the standing modes to represent traveling or propagating waves, a somewhat more complicated and arbitrary manner of separating the. variability y. Mathematically, the procedure of separation in CEOFs is similar to real EOFs (see Lorenz, 1956; Anderson 1963; Stidd, 1967) except that the [imc-avc.raged spatial covariance matrix is formed using a complex time series $I_p(x,y,t)$ (ser. Vazquez, 1991) where the real part is just the. time series at grid point (x,y) while the imaginary part is its Hilbert transform in time. Thus both the eigenvector $F_i(x,y)$ of the spatial covariance matrix and the temporal amplitudes $w_i(t)$ arc complex and have an amplitude and a phase component. The slope of the spatial phase can be interpreted as a wavelength since $\Delta\vartheta_s = k\Delta x$ or the wave.nuriihcr $k = -\frac{\Delta\vartheta_s}{\Delta x}$ while. the slope of the temporal phase can be interpreted as an instantaneous frequency since $\Delta\vartheta_t = \omega\Delta t$. Although useful, these quantities can be difficult to interpret when estimated from noisy data. For details and specific simulations done. using the CEOF approachsccVw/~uc.z(1991).

To derive the spatial and temporal phase information, CEOF analysis was applied to the 74 maps of gridded residual sca level between I)ecember 1, 1986 and November 30, 1988. The original 4 point per degree data set was subsampled to 2 points pcr degree of latitude and longitude in order to reduce the size of the. spatial covariance matrix necessary in the. CEOF calculation. The spatially correlated signal in the area between 35°N and 43°N and 75*W 1060" W (see Figure 1) was found 10 be dominated by the first four CEOFs. These first four CEOFs were found to explain nearly 60% of the variability with the first four mode.s accounting for 26%, 17%, 9%, and 7% of the. total variance., respectively. A plot of cumulative percent of variability explained versus mode # is shown in Figure 2. It is readily seen that higher mode.s add little variance to the total variability, as the modal structure becomes quickly

degenerate. Degeneracy in itself is not a sufficient condition for statistical insignificance and thus some type of further analysis is necessary to determine the. significance of the.sc four modes. A Monte-Carlo simulation (see Overland and Preisendorfer, 1982) analysis was applied to determine the. statistical significance of these modes (see Figure 3). The simulation indicated that the first four modes were above the 99% level of significance with none of the random modes explaining more than 4.7% of the variability.

Figure 4(a,b) shows the.tcrnlmtil amplitude and phase, for the first CEOF. For the. sake of plotting the temporal amplitude has been divided by the square root of the total number of grid points. The time variation of this mode shows a maximum toward the first year of the ERM. However, without examining the. phase, this quantity by itself is difficult to interpret. The frequency at a given time is equal to the slope of the temporal phase plot at that time. During the first year of the Geosat ERM (December 1986-November 1987), the first CEOF indicates that on the average a 1 cycle/year frequency was dominant. However, slopes for the second year of the ERM (December 1987-November 1988) are associated with higher frequencies. Figure 5(a,b) shows the spatial amplitude pattern and phase for this CEOF. For purposes of plotting the spatial amplitude has been multiplied by the. square. root of the total number of grid points. The spatial amplitude of the first CEOF shows that several local maxima exist at 37°N, 74*W; 38°N, 67° W; and 38°N, 64°W. A maximum also exists away from the Gulf Stream al 41°N and 69*W, The spatial phase is meaningful only at those locations where. the amplitude is high. These areas are highlighted by shading in Figure 5b. A disadvantage of CEOFs is the ambiguity and poor statistics involved in defining these maxima. Nonetheless, Figures 4 and 5 indicate that in those areas where local maxima in amplitude exist, the. phase. in the along-stream direction dots not change. rapidly, as the lines of constant phase are parallel to the mean path. Of course, discontinuities exist at 0° making the, interpretation of the phase difficult

The temporal amplitude and phase plots for the second eigenmode are shown in Figure 6(a,b). Relative to the. first CEOF, the. temporal amplitude. has decreased by approximately 33%. The slope of the temporal phase between December 1986 and July 1988 reveals a dominant 1 cycle/year frequency. Between July 1988 and December 1988 the phase behave.s in an almost random pattern. The spatial

amplitude and phase in Figure 7(a,b) indicate local maxima exist at approximately 37°N, 73*W; 39°N, 67"; 39° N, 64°W; 37°N, 63°W; and 42° N, 69°W. As an example the. spatial phase in two areas of high amplitude has been highlighted by shading. The spatial phase in these areas show that lines of constant phase are not as parallel to the Gulf Stream mean path as is the case with the first CEOF, suggestive of possible along-stream propagation. In addition the phase difference between these two highs is approximately 180°.

The temporal amplitude and phase for the third CEOF are shown in Figure 8(a,b). A maximum in the temporal amplitude of this CEOF occurs in December of 1987. Relative to the second CEOF, this maximum has about the same magnitude. The slope of the temporal phase plot seems to vary considerably during the two- year period indicating the presence of different frequencies in the CEOF. However, the. first year of the ERM for this CEOF is associated with an average frequency of 3 c.yc.lc.s/year. The spatial amplitude and phase for this CEOF, shown in Figure 9(a,b), indicate several amplitude maxima appear at 36.8°N, 73° W; 36.8°N, 68.5° W; 39°N, 66° W; 36.8°N, 61" W; and 40°N, 61 'W. As with the second CEOF the slope of the phase contour lines (see shaded regions) indicates along-stream phase propagation.

Shown in Figure 10(a,b) is the temporal amplitude and phase for the fourth CEOF. A maximum in amplitude occurs in approximately February of 198"/, The slope of the temporal phase is such that this CEOF, on the average, is associated with a frequency of 2-3 cycles/year. From Figure 11(a,b) the spatial structure of this CEOF reveals that most of the variance, is concentrated downstream of 65°W as well as the. ability of the CEOF analysis to detect regional patterns of coherence. A maximum in the. spatial amplitude, of this CEOF occurs at 38°N, 63° W. An example. of an area of high amplitude has been shaded in the phase plot (Figure 10h). Lines of constant phase (contours) in this area are. almost North-South, indicative. of the. along-stream propagation of this mode. Other phase contours in areas of low spatial amplitude arc meaningless due. to the low coherence of the. estimate of the. CEOF.

The spatial phase. plots of these four CEOFs bring out the difficulty in interpreting alrmg-stream phase propagation. The uncertainty of the estimate in areas of low spatial amplitude, as well as discontinuities at 360°, lead to problems of interpretation of the relevant space-time quantities for a given

CEOF. The problem can be made. easier by examination in some type of along-stream coordinate, reducing the. problem to two dimensions instead of three. In addition, the. reduction to an along-stream coordinate system allows for the application of wavenumber-frequency techniques which separate the variance into westward propagating, eastward propagating and stationary components. This may be accomplished by recreating the spatially correlated filtered time series for each CEOF and the.n averaging and subsampling spatially along the mean path of the Gulf Stream at 0.5 degree longitude intervals.

Generally since spatial highs in the CEOFs follow the. mean path of the Stream, the. averaging procedure used is a good representation of the. strut.turc. of the.CEOFs. However, as observe.d in the first 3 CEOFs, highs do exist which are off.set from the. mean path of the. Gulf Stream. As an example the second CEOF has highs at 37*N, 63° W as well as at 39*N, 64° W. As in the first CEOF, the. phase difference. across the Stream is approximately 180°. This phase difference may be accounted for by the derivation of the sea level residual from the mean sea level across the Stream (see Figure 12). Such a calculation, depending on the shape of the mean signal. leads to a high on one side of the Stream and a low orr the. other (see Kelley and Gille, 1990). Although a good representation, the. alor~g-Stream averaging in the CEOFs will not rc.prc.sent North-South propagation in the CEOFs or eddies which might be coherent with path displacements.

The data set that was used to dc.rive the mean path of the. Gulf Stream was bawd on charts of North Wall positions from the NOAA AVHRR (IR) satellite infrared sensors. These charts arc distributed by the Oceans Product Center/National Ocean Service Branch of the National Oceanic and Atmospheric Administration (NOAA/NOS/OPC). After digitizing the North Wall positions, a mean path between December 1, 19S6 and November 1988 was calculated. The only use of the AVHRR data in this study was in calculating the mean path.

Mathematically the CEOF filtered time series over the spatial domain is then recreated by multiplying the temporal part of the eigenmode with the complex conjugate of the spatial part. The real part of the rc.suiting expression represents the filtered time series for that CEOF. Using the. mean path data, an average sca level anomaly for the given CEOF time series was calculated over a 100km x 100km window spanning the mean path of the Gulf Stream at 0.5 degree longitude intervals. The rc.suit of this

subsampling and averaging procedure is a longitude-tinm contour plot of sca level anomaly for each CEOF. These results are shown in Figure 13 for CEOFs 1-4, respectively.

The first CEOF is associated with a quasi-stationary pattern whose pattern suggests a dominant frequency of 1 cycle/year (see Figure 13a). Between 75°W and 65°W and day 846 to 1065, there is evidence for westward phase propagation due to the. observation of highs in sea level anomaly at later times wiLh increasing upstream distance. An average slope, and thus phase speed on the order of 5 km/day, may be determined from the. line connecting highs at each time step. A maximum of 38cm occurs on day 919 at 63°W. The appearance of two complete cycles during the two-year period indicates the dominance of the annual cycle. A note.worthy feature, which will be analyzed further in the discussion section in connection with the New England Seamounts, is the. abrupt change in the shape and direction of the contours at 65°W. This quasi-stationary pattern is consistent with earlier results (Halliwell and Mooers, 1983) showing a standing wave in this region with a node at approximately 70°W.

The second CEOF (Figure 13b) is difficult to interpret as one. wave, but onc dots notice. a change. in the. slope of the contour line.s at 66°W. However, the. pattern is too complicated Lo identify clearly with onc dominant frequency or wavelength, although the appearance of two complete cycle.s indicates evidence for the annual cycle. The pattern appears to be onc associated with wave propagation both cast and west of approximately 67°W. The. amplitude maximum of 24 cm occurs between day 773 and 846 at 66° W.

The third CEOF (Figure 13c) contains more local highs and lows than either of the first two CEOFs suggesting that frequencies higher than 1 cycle./ycar may be involved. A maximum amplitude of 28 cm occurs on day 1357 at 60.5°W. A zero level in the. data appears at 67" W, indicating a change in the propagation properties of this CEOF.

The. appearance of several highs and lows (Figure. 13d) in the fourth CEOF suggests also that frequencies higher than 1 cycle/year are present, A maximum amplitude of 26cm appears on day 1138 at 63" W. Most of the variability y of this mode. occurs downstream of 65° W, The slope of the. line. connecting highs at successive times is indicative of westward phase propagation at approximately

4km/day. The location of the variability of this mode in an area of known eddy/Stream interactions (see Halliwell and Mooers, 1983) will be discussed further.

Figure 13e shows the longitude-time plot for the unfiltered data (before running CEOF analysis) averaged and subsampled along the mean path in the same way as the first four CEOFs. The dominant signal from the first CEOF is distinguishable, but the noisier plot dots not allow for identification of the other signals. The advantage of using the CEOF as a filter will become more evident in the next section as the wavenumber-frequency spectra of these longitude-time plots are examined.

In all cases, maximum amplitudes for these CEOFs appear to occur downstream of 67*W. This would coincide with the increase in meander amplitude observed in this area by Halliwell and Mooers (1983), Hansen (1970), and Cornillon (1986). Cornillon points out that the exact nature of the increase, whether linear or a step at the New England Seamounts, is uncertain. There is nothing in the longitude-time plots that suggests a smooth linear increase in residual sea level anomaly with downstream distance. Nonetheless, because of the one spatial dimension the longitude-time contours of residual sea level anomaly provide an opportunity for application of two-dimensional wavenumber-frequency techniques to observe what part of the variance in these CEOFs is due to propagating components or stationary components.

4. Wavenumber-Frequency Spectra

To determine the propagation and space.-timc characteristics of the first four CEOF modes, two-dimensional frequency-wavenumber spectral techniques were applied to the longitude-time plots. Using notation developed by Kao (1968), Tsay (19"/4), Hayashi (1971), and Pratt (1976) the space-time Fourier transform of a function 1 l(x,t) of longitude, (x) and time (l) can be de.fined as:

$$Q(k,\omega) = \frac{1}{4\pi^2} \int_0^{2\pi} \int_0^{2\pi} H(x,t) e^{-i(kx + \omega t)} dx dt, \qquad (2\text{-}8)$$

where "x" is the longiludc.coordinate with positive being eastward and ncgalivc.being westward. in an area such as the. Gulf Stream where phase propagation is thought to exist in both the westward and eastward direction, the two-dime.nsional wavenumber frequency spectrum allows one. to separate the variance into westward, eastward and stationary components.

The two-dimensional analysis used here will identify as propagating variance (eastward or westward) the difference between the variability due to eastward and westward propagating waves in a given frequency - wavenumber band. The remaining variability, or that part of the variance. common 10 both waves, is identified as stationary wave. activity, However, for this variability to be a measure of true standing wave activity, the eastward and westward propagating waves must be correlated in time or the coherence (γ) between the two waves must be high. Hayashi (1971) shows that for the coherence between an eastward and westward propagating wave to be high, the coherence between the time dependent Fourier coefficients must be high. Thus this coherence (y) can be used as a measure. of the statistical significance of the. stationary wave. activity. The measure of standing wave activity is then dependent on this statistical significance. One advantage of applying two-d imensional wavenumber-freq uency techniques to the CEOFs instead of the original time series is the spatial correlation of the CEOFs. Thus one expects that coherences for these modes should be high. For further details on these techniques see Vazquez (1991). In all cases, be fore FFTs were calculated, the data were cosine-tapered over the first and last 10% with a linear trend and bias taken out to remove, the long-period trend (Bendat and Piersol, 1971).

Figure 14 contains the spectral plots for the first four CEOFs and shows what part of the total variance in these CEOFs is associated with propagating and stationary variance. The total variance for a give.n

wavenumber-frequency band would be the sum of the.sc two components. All the spear-al plots have been smoothed over three frequency bands and three wavenumber bands to gain statistical confidence in the coherence estimates. The smoothing was a running band average in both wavenumber-frequency space, thus individual spectral estimates are not independent of each other, The averaging process leads to 18 degrees of freedom. However, coherence estimates were based on 14 degrees as smoothing was applied over only seven bands in the. frequency domain (see Hayashi, 197 1; Pratt, 1976). The convention used in these plots is that for propagating variance, negative or dashed lines indicate eastward propagation while. positive. or solid lines indicate westward propagation.

The propagating variance in CEOF 1 (Figure 14a) is separated into two distinct wavenumber- frequency bands. A westward propagating component is centered in a frequency band between 0.S cycles/year -1,5 cycle.s/year and a wavelength of approximately 1400 km. The eastward propagating component is more broad-banded with respect to wavelength, with energy existing between 300km and 1400km. These two peaks arc not, however, statistically different at the. 95% level of confidence. There is a considerable amount of energy (approximately 60% of the variability is associated with stationary wave activity and 40% propagating) in the stationary wave spectrum (Figure 14 b), and as expected the coherence of 0.98 is above the 99% level of statistical significance (0.70) for 14 degrees of freedom.

The second CEOF (Figure 14c) appears to be more trroad-banded in wave.number space with eastward propagating variance occurring in a band between 300km - 1400km and 0.S cycles/year -2.0 c.yclcs/year. The. stationary wave spectrum contains 70% of the total energy with a coherence of 0.89. Once again, the coherence is consistent with true standing, wave. activity.

The third CEOF (Figure 14(e,f)), like the, first, contains variance due to both westward and eastward propagating components. Structurally it is similar to the first CEOF except the energy is contained in a frequency band around 1.5-2.0 cycles/ycw instead of 1 cycle/year. The amount of energy in the stationary wave. spectrum and the propagating wave. spectrum is approximate.ty equally distributed (SO% each) with a coherence of 0.98 indicative. of standing wave. activity. The redness of the. spectra for the first three CEOFs suggest that both interannual and long-wavelength variability exist which is not being rc.solved by the two-ycar ERM Geosat data set.

The spectra for the fourth CEOF (Figure 14(g,h)) are not as red as the first three CEOFs indicating that the two-year data set of sea level anomaly is sufficient to completely resolve this eigenmode. Energy is contained in a band between 500km - 700km and 2-3 cycles/year. The positive sign of the propagating variance spectrum implies westward phase propagation which is clearly evident also in Figure 13d (see slope of line connecting highs). The propagating variance spectrum accounts for approximately 60% of the total variance, v'hilt, the stationary wave spectrum, accounts for 40% of the total variance and has a coherence of 0.99.

Figure 14(i,j) shows the spectra for the. unfiltered sea level data (Figure 13e), averaged and subsampled along the mean path in the same way as the first four CEOFs. The propagating spectrum is clearly dominated by eastward propagation with westward propagation occurring only in a few bands centered at wavelengths around 1400km. In addition, the coherence for the. slat ionary wave spectrum is 0.25 indicating that even though there is a siginficant amount of energy in the spectra, showing the presence of both eastward and westward phase propagation, the stationary spectrum (about 50% of the total energy) does not represent true standing wave activity. These. results indicate how the CEOF analysis can behave effective.iy as a filter, making it easier to interpret a noisy data set. In addition individual CEOFs are spatially coherent, which explains the high coherences associated with the stationary spectra in the CEOFs and the iow coherence associated with the. unfiltered data set.

The results presented here. show that even at the long periods, the Gulf Stream exhibits motion over a wide range of wavelengths and lime. Although the identification of these waves with specific dynamics is difficult because of the complexity of the Gulf Stream due. to high relative vorticity, nonlinear terms, and possible coupling between layers, a scaling analysis of topographic waves, along with some simple comparisons with current thin-jet barotropic models and previous observations can lend some insight into the physics of these modes. It is important, however, to remember that the statistical nature of the study does not guarantee a physical explanation or cause for each eigenmode, oniy that each mode is orthogonal and uncorrelated with others. Therefore, comparison of these results with others is valid oniy for domains of the same size, along with identical temporal and spatial resolutions. in addition, these spectra rcprc.sent only the behavior of the CEOF modes along, the mean path of tire Gulf Stream.

5. Discussion

Although the CEOF technique separates the. variance into different modes based on statistics and not dynamics, the scales of motion of these CEOFs as well as the observed change in wave,-]ikc, structure between 67*W and 65° W can provide. some insight into what mechanisms might be influencing the.sc long-period oscillations of the Gulf Stream. Besides the changes in the wave-like structure which occur between 67"W anti 65°W, for CEOFs 1 and 3 waves longer than approximately 1400km propagate westward while shorter waves propagate eastward. Two possible mechanisms will be examined to explain the.sc strong trends in the. CEOFs. One deals with the appearance of the. Ncw England Seamount chain in the area downstream of 67*W. The trend for longer wavelength structures to propagate westward and those shorter to propagate eastward wiii be examined in the. context of a recent thin -jet barotropic model (s c c Cushman-Roisin et al., 1992). Downstream of 65°W, eddy/Strcan] interactions (see Halliwell and Mooers, 1983) may also be a large factor in determining the Stream dynamics. Thus Cl;CW'4 wiii be examined with respect to the effect eddy/Strcan~ interactions downstream of 65°W may be having on its structure.

The trend for longer wave.icngtils to propagate westward and shorter wave.icngths to propagate cast ward is consistent with a recent barotropic thin-jet model (Cushman-Roisin et ai., 1992). Such mode.ls have been used in the past in an attempt to explain the meandering of the Gulf Stream along with the in fluence of eddy/dctachn~cnt processes on this meandering. 1 lowever, the first thin-jet models (see Warren, 1963; Robinson and Niiler, 1967) were steady-state and were not able to predict the propagation properties of the.scmeanders. The assumption in these models, that the width of the, jet is much smaller than the radius of curvature, allows for the Jacobian of the coordinate transformation to a set of Stream co.ordinate.s to be solved. Employing a 11/2 layer model, while including the nonlinear advection terms and time dependence, Cushman-Roisin et. al. (1992) were able to determine a critical wavelength at which the westward propagation tendency associated with Rossby waves balances the eastward propagation associated with advection and the local vortex induction

produced by the curvature of the Stream path. Scaling the. equations with the proper parameters for a jet like the Gulf Stream they determined the critical wavelength was around 1130km, Although lower than that observed in our CEOF analysis, it is comparable with the first and second CEOFs which appear to indicate. a critical wavelength of 1400km. However there arc. several possible reasons for the observed differences. 't he observed spectra from the Geosat al timeter data, because of the sampling rate of 1 point every 17 days (with a 3-day subcycle) will bc aliased, since meanders are energetic for all periods greater than four days (see Watts and Johns, 1982). in addition the size of the domain (approximately 1500 km) is not sufficient to rc.solve these long-wavelength fluctuations. Thus the spectra are aliased in both time and space., certainly influencing the calculation of the. critical wavelength. The thin-jet model is also a 11/2 layer barotropic model (bottom layer at rest), unlike. the Gulf Stream which is observed to have. both a strong barotropic and baroclinic signature (e.g., Halkin and Rossby, 1985). Considering the lack of a sufficiently long data set in both space and time to resolve these meanders, as well as not taking into account the baroclinic structure of the. Gulf Stream in the mode.t, the. comparison between model and observations is encouraging. }lc.sides the baroclinic structure which is missing in the thin-jet formulation, it also does not take, into account topographic effects such as those duc to the. New England Seamounts. A simple examination of the. gradient of topography found in the region along with the appropriate scaling of the topographic dispersion relationship can lend some insight as 10 whether topography might be responsible for the changes in the wave-like. structure observed at approximately 65°W.

From Pedlosky (1979) the topographic dispersion relationship for a one-dimensional wave traveling in the renal direction with a meridional bottom slope is

$$\sigma = -\frac{f_o}{D}\frac{\partial h_b}{\partial y}\frac{1}{k} \qquad (1)$$

where

f.= the Coriolis parameter at approximately 40°N

D=- approximate depth of the water column

$\frac{\partial h_b}{\partial y}$ is the slope Of the bottom topography

k is the zonal wavenumber.

In terms of the geographic location of the.sc seamounts relative to the mean path as determined by averaging the bathymetry in a 100km x 100km square box spanning the mean path of the Gulf Stream, Figure 15(a,b) was plotted to illustrate the in fluence of the. New England Seamounts in the given area. Figure 15b was generated by doing an averaging at the 0.S longitudinal degree intervals. For this give.n resolution, the plot clearly indicates a change, in the. gradient of the bathymetry observed at 67° W. Due to the symmetry of the Ncw England Seamounts, onc may assume that the along-Stream gradient is representative of the. meridional bottom slope. From Figure 15 the change in bathymetry between 67*W and 65° W is approximate.ly ?000 meters while the along-stream distance is 170km giving a seal ing value 0.01 for the meridional slope, At 40°N the Coriolis term is equal to $1.5e^{-5}$/sec. Thus the influence of topography when compared to the Beta term (in the barotropic sense) can be dc.rived as

$\frac{f_0}{D}\frac{\partial h_b}{\partial y} \backslash \beta$, which in this case is on the order of 10. However, the. importance of the baroclinicity of the Stream can be seen in the dispersion relationship where, for a wavelength of 1500km, the derived frequency from the barotropic dispersion relationship in (1) is on the order of 10 cycles/year, higher than our observed frequency of 1 cycle/year. Thus, although topography might have an effect on the ob.served waves, stratification and the. baroclinic structure of the Stream could be very important, especially in the first three CEOFs where, the. annual cycle is dominant. However, as long as the. wavelength is greater than the internal Rossby radius of deformation the effect due. to stratification is minimal (Pedlosky, 1979). In addition to this simple scaling analysis there is evidence for the Gulf Stream not being critically controlled topographically by the Ncw England Seamount chain, Pratt

(1989) shows that, for upstream wave propagation upstream of the New England seamount chain, the. path envelope width should decrease downstream of the topographic influence. However, there is no evidence suggesting that this is the case in the Gulf Stream, which is known to wide.n as it goes downstream (see Cornillon, 1986).

An important point to be made is that the wavenumber-frequency spectra indicate an average spectrum over the spatial domain. They give no information as to spatially where the eastward or westward propagation is occurring. Such information may be derived from the longitude time-plots (Figure 13). For the first CEOF eastward propagation is identifiable downstream of the seamounts, but not upstream. The second CEOF appears to contain both westward and eastward phase propagation upstream of the seamounts and eastward propagation downstream of the. Seamounts. The propagating spectrum of this CEOF (Figure 14(c,d)) indicates no westward propagation, but the. stationary spectrum contains 70% of the energy, indicating that westward propagation may be identified within the, context of a standing wave pattern.

Although the first three CEOFs are energetic over the entire domain of study, the fourth CEOF is different in that a significant percentage of its variability is concentrated downstream of 65°W. The spatial pattern of the CEOF (see Figure 11) indicate.s that the, variability is concentrated in an area which is known to be associated with eddy/Stream interactions (see Richardson, 1980; Halliwell and Mooers, 1983). It is worth comparing the propagation properties of this mode with models of the Gulf Stream which reproduce interactions of eddies with the Stream path.

The westward phase propagation observed in CEOF 4 is characteristic of Gulf Stream models where the Stream is treated as a potential vorticity front and eddies as point vorticities. Such a model used by Stern and Flierl (1987) produced a retrograde propagation (with respect to Gulf Stream) of 2.5km/day. This is smaller than the 4 km/day phase speed calculated using $c_p = \frac{\omega}{k}$, where. ω and k arc. taken from the propagating spectrum to be 15.7 radians/year and 0.01 radians km"], respectively. The discrepancy could indicate, that if eddy/Stream interactions are. responsible for the. structure. of this CEOF, displacements in the Stream do not propagate at the same speed as the eddies. However, the

4 km/day phase speed dots compare well with an average propagation speed of 5 km/day calculated by Richardson (1980) for eddies in this area. Nonetheless, as pointed out by Stern and Flierl (1987), west ward propagation is oh.served during the. eddy/detachment process. This, along with observations by Halliwell and Moot.rs (1983) of eddy/Strc.an] interactions downstream of 65°, indicates the possibility of the. fourth CEOF mode being influenced by such events.

6. Conclusions and Summary

Using the. technique of Complex Empirical Orthogonal Functions (CEOF) in the Gulf Stream region between 35°N and 43" N, the variability of sea level was separated into uncorrelated and orthogonal propagating modes. The first four complex empirical orthogonal modes in the area between 35°N and 43" N and 75"W to 60° W were found to be statistical] y significant at the 99% level of confidence. These four modes accounted for approximately 60% of the variability. In all cases, some type of deflection or change in the observed wave-like patterns was evident between 66"W and 63° W. The deflection in the wave.-likc patterns in an area downstream of 67°W is located where the meandering of the Gulf Stream should be influenced by the New England Seamounts. A simple scaling of the barotropic topographic dispersion relationship indicates that the topographic effect is as large. as the Beta effect. Since the scaling argument was based on the barotropic formulation, a conclusion about the relative importance of the beta and topographic terms in a barotropic sense indicates only that topography could be important, with strati fic.alien decreasing the importance of the topographic term.

The relevant space.-tirnc scales and propagation properties of the first four modes were identified by applying two-dimensional wavenumber-frequency spectral techniques to spatially subsampled longitude-time plots. The first and third modes were, associated with both westward and eastward propagating waves. The westward propagation associated with the first mode has a wavelength greater than 1400km at a frequency of 1 cycle/year. The phase speed of the westward propagating wave was calculated to be approximately 5km/day. A shorter 500 km wave.lcnglh component propagated cast ward at 1 cycle/year. Variance in the second CEOF was duc to both eastward propagation and standing wave activity over a broad wavenumber band between 1400 and 300km and a frequency centered at 1 cycle/year. The third CEOF was similar in structure to the first except that it was associated with a higher frequency between 1.5 and 2.0 cycle/year. The trend in the first and third CEOFs for longer wavelengths to propagate westward and shorter ones eastward is consistent with thin-jet mode.]s which indicate, a critical wavelength of 1130. This critical wavelength is a measure of w'here the tendency for westward

propagation due to Rossby wave, propagation is balanced by the tendency for eastward propagation associated with advection and a local vortex induction duc to the curvature of the Stream path.

The fourth CEOF is unique in that its variability is contained in an area downstream of 65°W. The spatial pattern of this CEOF is indicative of possible eddy/Stream interaction as a contributing mechanism to its structure. The phase speed of 4km/day is consistent with earlier results of eddy propagation speeds. However, direct comparisons arc difficult because there is no theoretical evidence to suggest that displacements of the Stream path due. to possible eddy/Strc.am interactions propagate. at the same sped as the eddies.

These results point out that even at long time scales, the response of sca level in the area of the Gulf Stream is most like.ly duc to several factors. Although the scales of motion discussed in this research approximate those of an annual baroclinic Rossby wave, the complexity of the Gulf Stream duc to nonlinearities and topography make direct mode.1/observation comparisons difficult.

The CEOF technique has prove.n to be a valuable tool in filtering out the long-period spatially correlated signal. As a next step in this research, it would be useful to run similar CEOF analysis on global eddy resolving ocean circulation models in the area of the Gulf Stream (see Malanotte-Rizzoli et al., 1990; Thompson cl al., 1990). As a first step the domain of the study needs to be enlarged to adequately resolve tbc 2000km wavelength associated with the first CEOF. This could provide some insight into the. physics of this first mock.

Acknowledgments

The author would like to thank Lee-Lueng Fu, Victor Zlotnicki, Mike Freilich, Claric Perigaud and Ichiro Fukumori at the Jet Propulsion Laboratory for many invaluable discussions concerning this work, Two reviewers provided many helpful comments on how to improve the work. Tom Dickey at the University of Southern California also provided many useful discussions. Akiko Hayashi is thanked for her part in processing the Geosat data and Jennifer Clark at NOAA is gratefully acknowledged for her analysis of the Gulf Stream charts. Lee Johnson at the image processing lab at the Jet Propulsion Laboratory was extremely helpful in the process of digitizing the Gulf Stream North Wall positions from the NOAA charts. Support is also acknowledged from the JPL-Cray supercomputer. The work was carried out at the Jet Propulsion Laboratory, California Institute of Technology under contract with the National Aeronautics and Space Administration. Partial support from the TOPEX/POSEIDON Project through a NASA Anouncement of Opportunity is also acknowledged. The final revisions were completed while a visiting scientist at the Instituto de Ciencias del Mar in Barcelona, Spain.

REFERENCES

Anderson, T. W., Asymptotic theory for principal component analysis, *Annuls of Mathematical Statistics*, **34**, *122-148, 1963.*

Barnett, T. P., Interaction of the monsoon and Pacific Trade Wind System at interannual time scales, Part I: The equatorial zone, *Monthly Weather Review,* **11, 756-773, 1983.**

Bendat, J. S, and A. G. Piersol, *Random Data: Analysis and Measurement Procedures*, **407 pp., Wiley-In[crscicncc, New York, N. Y., 1971.**

Born, G. }1., J. L. Mitchell, and G. A, Heyler, Geosat ERM-Mission design, *J. Astron. Sci.*, **3s(2), 119-134, 1987.**

Bratseth, A, M., Statistical interpolation by means of successive corrections, *Tellus*, **38,439-447, 1986.**

Cheney, R. E., Comparison data for Seasat altimetry in the. western North Atlantic, *J. Geophys. Res.*, **87**(c5), **3247-3253, 1982.**

Cornillon, P., The effect of the Ncw England Seamounts on Gulf Stream meandering as observed from satellite IR imagery, *J. Phys. Oceanogr.*, *16,386-389, 1986.*

Cushman-Roisin, B., L. Pratt and E. Ralph, A general theory for equivalent barotropic thin jets, in press, *J. Phys. Oceanogr.*, *1992.*

Flierl, G. R., P. Malanotte-Rizzoli and N. J. Zabusk y, Nonlinear waves and coherent structures

in barotropic P-plane jets, *J. Phys. Oceanogr.*, 17, 1408-1438, 1987,

Fu, 1,.-1,., J. Vazquez, and M. E. Parke, Seasonal variability of the Gulf Stream from satellite. altimetry, *J. Geophys. Res.*, 92 (C1), 749-754, 1987.

Fuglister, F. C., Cyclonic rings formed by the Gulf Stream 1965-1966, in *Studies in* I.., *Physical Oceanography: A Tribute to George Wust on* his *80th Birthday, vol. 1,* edited by A. Gordon, pp. 137-168, Gordon and Breach, New York, N. Y., 1972.

Greatbatch, R. J. and A. Goulding, Seasonal variations in a linear barotropic model of the. North Atlantic driven by the Hellerman and Rose.nstcin wind stress field, *J. Phys. Oceanogr.*, 19, $72- S95, 1989,

Halliwell, G. R. and C. N. K. Mooers, Meanders of the. Gulf Stream downstream from Cape Hatteras, *J. Phys. Oceanogr.*, 13, *1275 -1292., 1983.*

Halkin, D., and 1'. Rossby, The structure and transport of the Gulf Stream at 73°W, *J. Phys. Oceanogr.*, 15, 1439-1452, 1985.

Hansen, D. V., Gulf Stream meanders between Cape Hatteras and the Grand Banks, Deep *Sea Research, 17, 495-511, 1970.*

Hayashi, Y., A generalized method of resolving disturbances into progressive and retrogressive waves by space Fourier and time cross-spectral analysis, *Journal of the Meteorological Society of Japan, 49, 425-428, 1971.*

Herrmann, P. and W. Krauss, Generation and propagation of annual Rossby waves in the North Atlantic, *J. Phys. Oceanogr.*, *19, 727-744, 1989.*

Horel, J. P., Complex principal component analysis: Theory and examples, *Journal of Climate and Applied Meterology*, *23, 1660-1673,* 1984.

Ikeda, M., Meanders and detached eddies of a strong eastward- flowing@ using a two-layer quasi-geostrophic model, *J. Phys. Oceanogr.*, *11, 526-540, 1981.*

Kelley, K. A. and S. T. Gille, Gulf Stream surface transport and statistics at 69"W from the Geosat altimeter, *J. Geophys. Res.*, 95(C3), 3149-3161, 1990.

Kao, S.-K., Governing equations and spectra for atmospheric motion and transports in frequency wavenumber space, *J. Atmos. Sci.*, 25, 32-38, 1968.

Lorenz, E. N. *Empirical Orthogonal functions and statistical weather prediction, Report* 1, Statistical Forecasting Project, MIT, 49 pp., 1956.

Malanotte-Rizzoli, P., Application of SYNOP and Geosat data with a primitive equation mode.1 of the Gulf Stream, *EOS trans., 71 (43),* 1404, 1990.

Overland, J. E., and R. W, Preisendorfer, A significance test for principal components applied to a cyclone climatology, *Mon. Wea. Rev., 110,* 1-4, 1982..

Pedlosky, J., *Geophysical Fluid Dynamics, 62.4* pp., Springer-Vcrlag, New York, N. Y., 1979.

Pratt, R, W., The interpretation of space-time spectral quantities, *J. of the Atmos. Sci.*, 33, 1060-1066, *1976.*

Pratt, L. J. and M. E. Stern, Dynamics of potential vorticit y fronts and eddy detachment, *J. Phys. Oceanogr.*, 16, 1099-1118, 1986.

Richardson, P.L., Gulf Stream ring trajectories, *J. Phys. Oceanogr., 10,* 90-104, 1980.

Robinson, A. R. and P. P. Niiler, *The theory of free inertial currents,* Tellus, 19, 269-291, 1967.

Stidd, C. K., The use. of eigenvectors for climatic estimates, *Journal of Applied Meteorology, 6, 255-264,* 1967.

Stern, M. E. and G. R. Flierl, On the interaction of a vortex with a shear flow, *J. Geophys. Res.*, 92(C1O), 10733-10744, 1987.

Thompson, J. D., J. 1,. Mitchell, and D. W. Blake, Iikidy-Mean energetics in the Gulf Stream during REX: Model/data intercomparison, *EOS trans.*, 71 (43), 1403, 1990.

'May, C.-Y., A note on the methods of analyzing traveling waves, *Tellus*, 24,412-415, 1974,

Tracey, K. L. and D. R, Watts, On Gulf Stream meander characteristics near Cape Hatteras, *J. Geophys. Res.,91* (C6), 7587-7602, 1986.

Vazquez, J., V. Zlotnicki and L.-L. Fu, Sca level variability it-s in the Gulf Stream between Cape

Hatteras and 50°W: A Geosat study, *J. Geophys. Res.*, 9S(C1O), 17957-17964, 1990.

Vazquez, J. , *Observations of the Long-Period Variability of the Gulf Stream Downstream of Cape Hatteras*, P.H.D. dissertation, University of Southern California, Los Angeles, Ca., 137pp., 1991,

Warren, B. A., Topographic influences on the path of the Gulf Stream, *Tellus*, 1 S, 167-183, 1963,

Watts, D. R, and W. E. Johns, Gulf Stream meanders: Observations on propagation and growth, *J. Geophys. Res.*, 87(C12), 9467-9476, 1982.

Worthington, L. V., On the North Atlantic Circulation, 110 pp., Johns Hopkins University Press, Baltimore, Md., 1976.

Zlotnicki, V., A. Hayashi, and L.-L. Fu, The JPL-OCEANS-8902 version of the Geosat altimetry data, *JPL internal Document* D-6939, 47 pp., Jet Propul. Lab., Pasadena, Ca., 1989a.

Zlotnicki, V., L.-L. Fu, and W. C. Patzert, Seasonal variability in global sea level observed with Geosat altimetry, *J. Geophys. Res.*, 94(C12), 17959-17969, 1989b.

Zlotnicki, V., Sea level differences across the Gulf Stream and Kuroshio Extension, *J. Phys. Oceanogr.*, 21, 599-609, 1991.

FIGURE CAPTIONS

1. Ground tracks for ascending Geosat passes in the Gulf Stream.

2. Cumulative percent variability explained by complex empirical orthogonal mode versus mode #. Only first 15 modes are shown.

3. Histogram and cumulative percentage of all eigenvalues greater than 3.0 for 100 simulation runs of CEOF analysis using a Gaussian random number generator. Approximately 761 such eigenvalues were identified.

4. (a) Temporal amplitude for first CEOF. Amplitude values have been divided by the square root of the total number of grid locations. Time axis is in days from January 1, 1985. Resolution is 1 point every 10 days.

(b) Temporal phase for first CEOF. instantaneous slope is a measure of the frequency at that instant in time.

5. (a) Spatial amplitude for first CEOF. Spatial amplitude has been multiplied by the square root of the total number of grid locations. Local highs are marked by the letter "H", Resolution is 4 points per degree of latitude and longitude, Contour interval is 0.5.

(b) Spatial phase for first CEOF. Instantaneous slope is a measure of the wave-number at a given grid location. Shaded areas are examples of where the spatial amplitude is high,

6. (a,b) same as Figure 4 except is for second CEOF

7. (a,b) same as Figure 5 except is for second CEOF

8. (a,b) same as Figure 4 except is for third CEOF

9. (a,b) same as Figure 5 except is for third CEOF

10. (a,b) same as Figure 4 except is for fourth CEOF

11. (a,b) same as Figure 5 except is for fourth CEOF

12. Ilustrates 180° spatial phase difference associated with removal of mean sea level across the Stream.

13. (a) Longitude-time contour plot for time series of first CEOF averaged and subsampled within a 100km x 100km box along the. mean path of the Gulf Stream. Contour interval is 5 cm. Dashed lines indicate negative sca level residual values while solid lines indicate positive values. Temporal resolution is onc point every 10 days while spatial resolution is 2 points every degree of longitude. Slope of solid line illustrate.s speed and direction of propagation of the wave.

(b) same as (a) except for second CEOF

(c) same as (a) except for third CEOF

(d) same as (a) except for fourth CEOF

(c) same as (a) except for unfiltered data set and contour interval is 20 centimeters

14. (a) Wavcnumbcr-frequency spectral plots for first CEOF showing the propagating variance in cm* *2. Each estimate is associated with 18 degrees of freedom.

Positive values or solid line indicates westward propagating variance and negative or dashed line indicates eastward propagating variant.c.

Vertical lines arc indicative of changes in the direction of propagation.

(b) Stationary variance in cm**2 for first CEOF. Contour interval is 0.25 with each estimate associated with 18 degrees of freedom.

(c,d) same as (a,b) except is for second CEOF

(e,f) same as (a,b) except is for third CEOF

(g,h) same as (a,b) except is for fourth CEOF

(i,j) same as (a,b) except for unfiltered data set

14. (a) Gulf Stream mean path, as derived from NOAA AVHRR charts for the same period of time as the Geosat ERM, superimposed on bath ymetry. Black solid line is the mean path of the Gulf Stream. Bathymetry is contoured at 500 meter intervals at a resolution of 12 points per degree.

(b) Bathymetry from (a) averaged within a 100km x 100km box spanning the mean path of the Gulf Stream at intervals of 0.5 degrees of longitude.

15. (a) Mean path as derived from NOAA charts superimposed on bathymetry contours within the study area.

(b) Average depth within a 100km x 100km box spanning the mean path of the Gulf Stream. Clearly indicates change of gradient at approximately 65W.

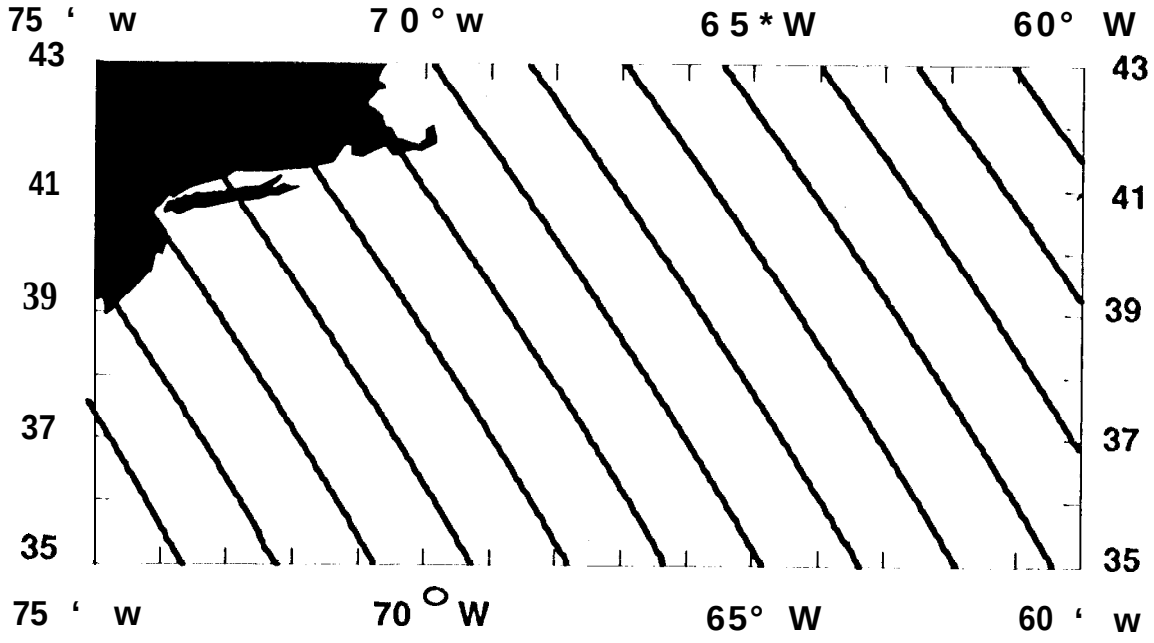

Figure 1

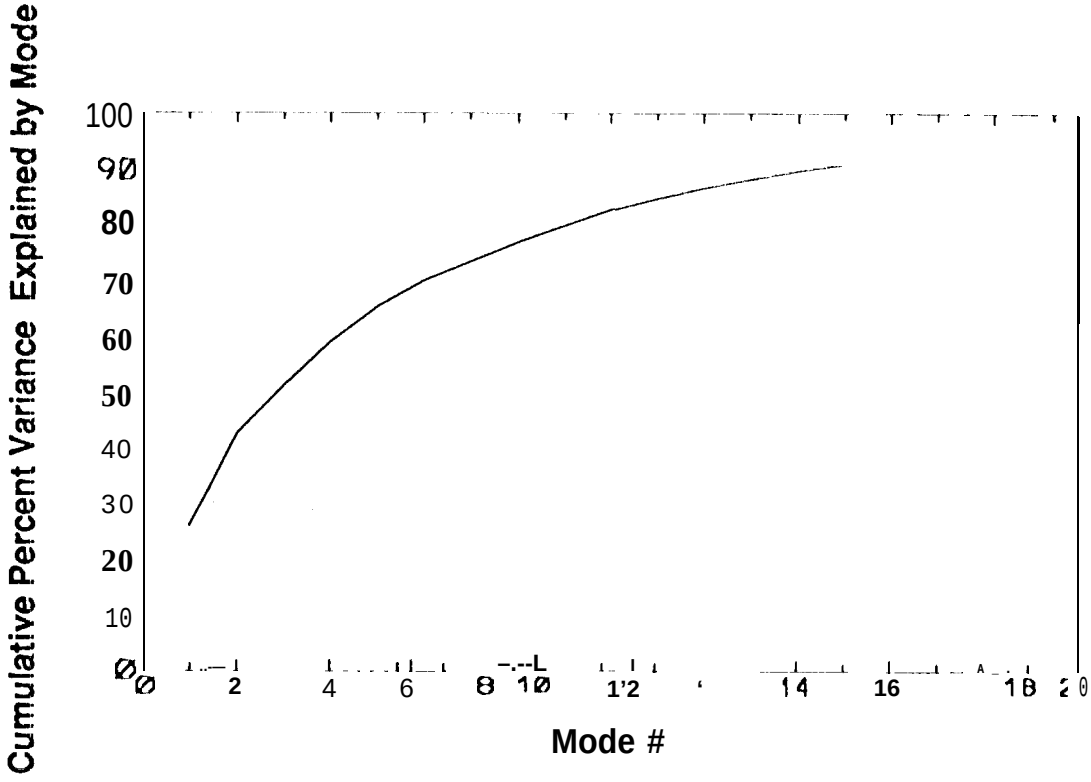
Cumulative Percent Variance Explained by Mode
100
90
80
70
60
50
40
30
20
10
0
0
2
4
6
8
10
12
14
16
18
20
Mode #

Figure 2

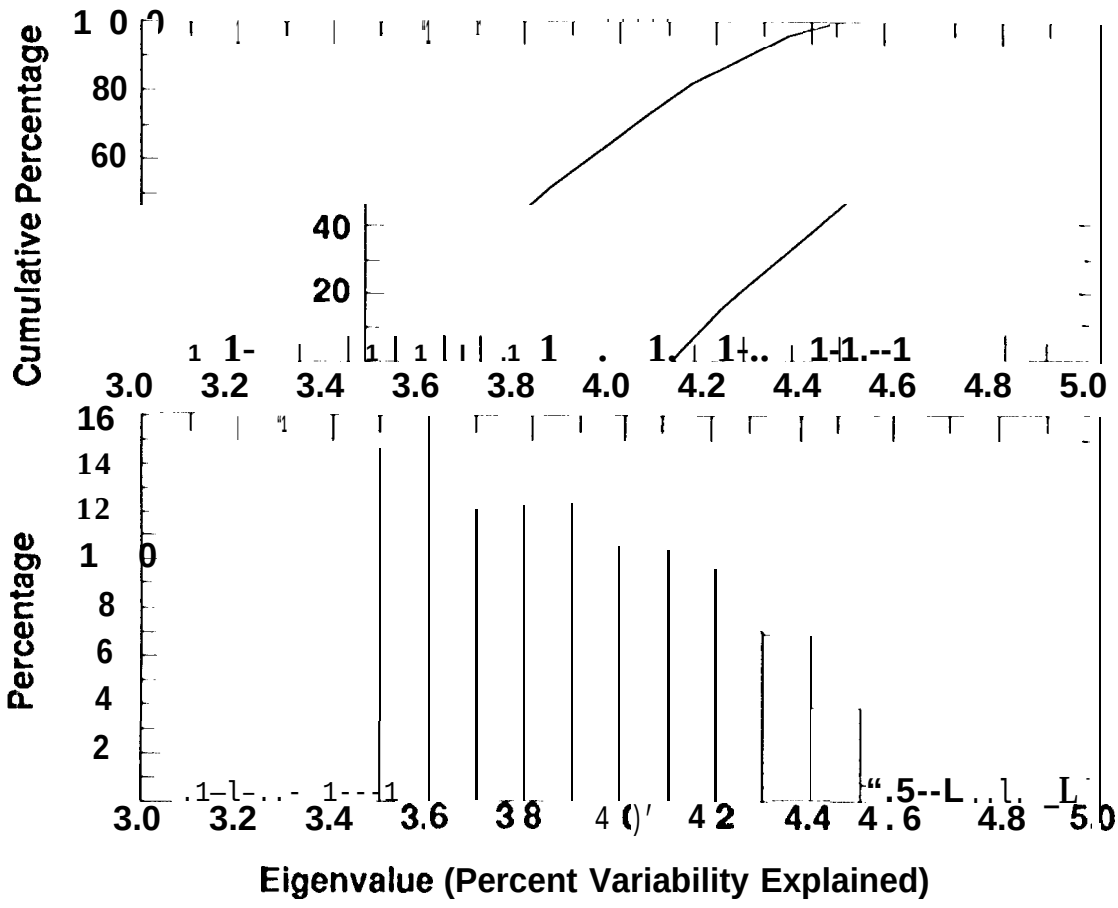
Cumulative Percentage
100
80
60
40
20
3.0
3.2
3.4
3.6
3.8
4.0
4.2
4.4
4.6
4.8
5.0
Percentage
16
14
12
10
8
6
4
2
Eigenvalue (Percent Variability Explained)

Figure 3

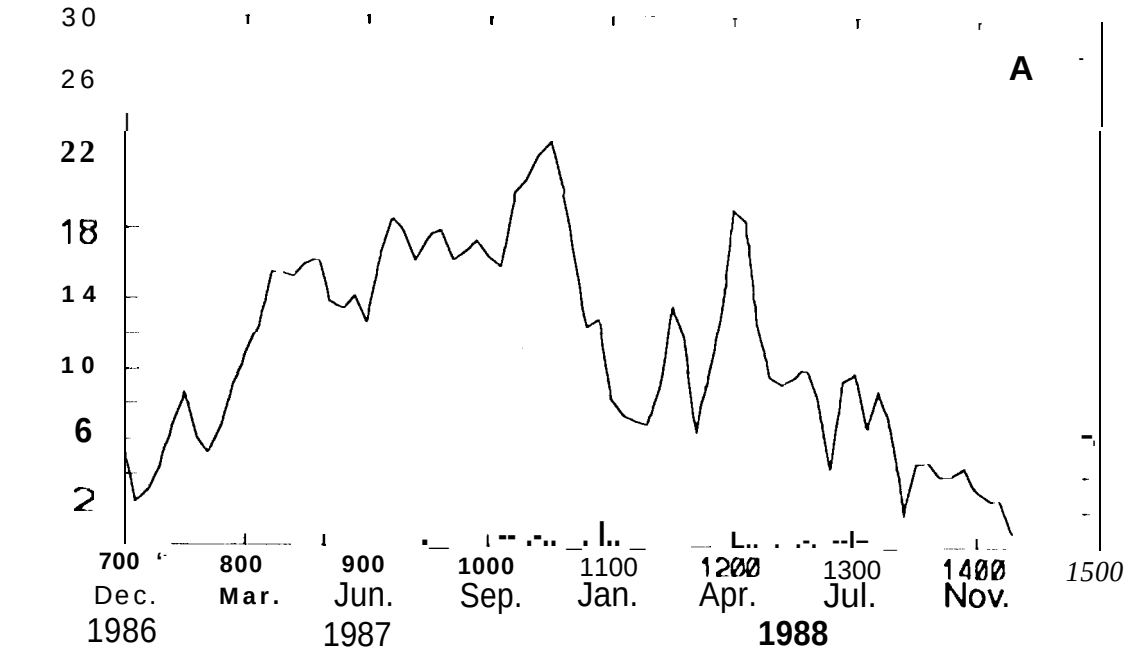
30
26
22
18
14
10
6
2
A
700
800
900
1000
1100
1200
1300
1400
1500
Dec.
Mar.
Jun.
Sep.
Jan.
Apr.
Jul.
Nov.
1986
1987
1988
Time in days

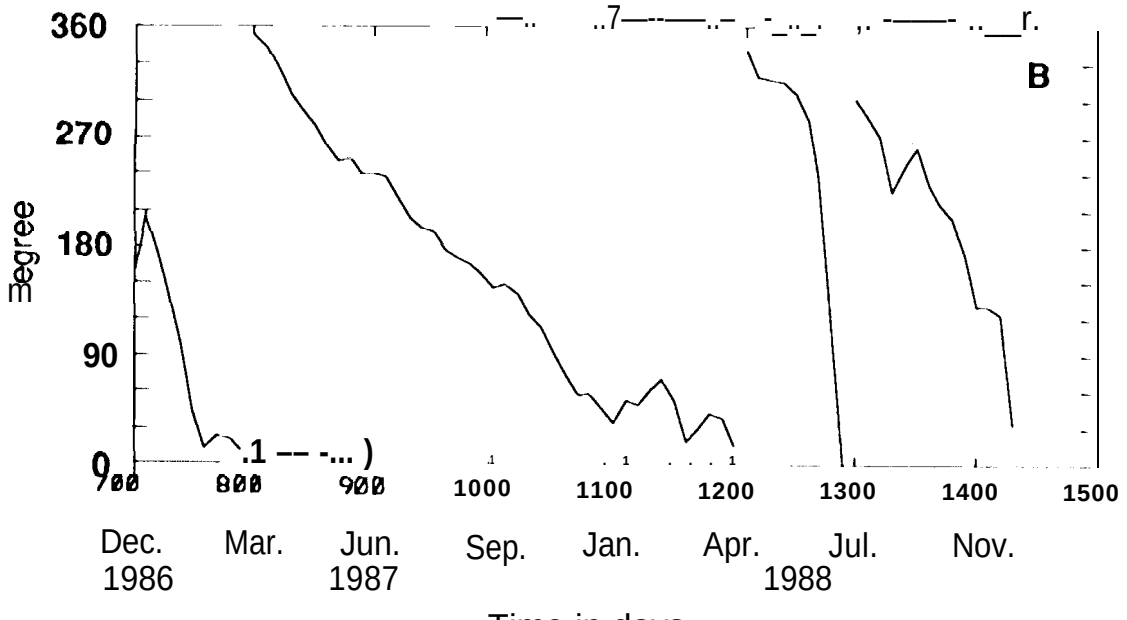
360
270
180
90
0
B
700
800
900
1000
1100
1200
1300
1400
1500
Dec.
Mar.
Jun.
Sep.
Jan.
Apr.
Jul.
Nov.
1986
1987
1988
Time in days

Figure 4

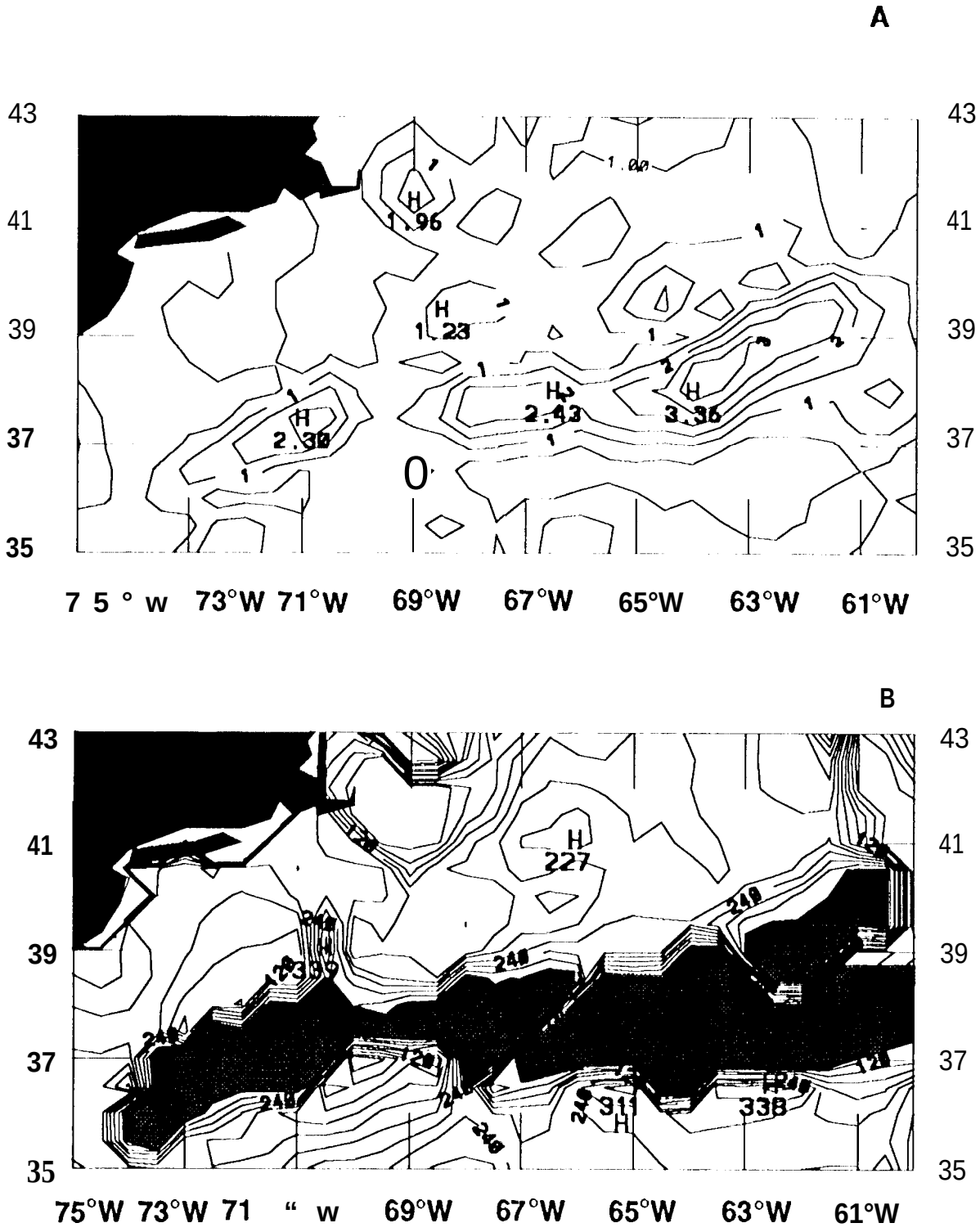
A
43
41
39
37
35
1.96
1.23
2.43
3.36
2.30
1.00
75°W 73°W 71°W 69°W 67°W 65°W 63°W 61°W
B
43
41
39
37
35
227
338
75°W 73°W 71 " w 69°W 67°W 65°W 63°W 61°W

Figure 5

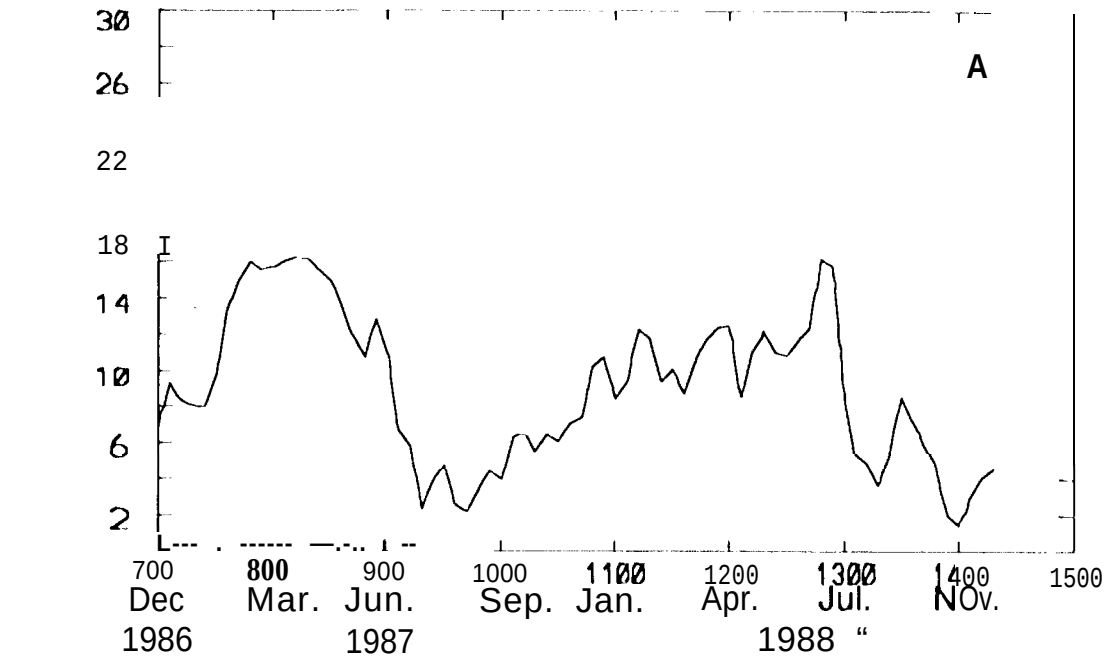
30
26
22
18
14
10
6
2
A
700
800
900
1000
1100
1200
1300
1400
1500
Dec
1986
Mar.
Jun.
1987
Sep.
Jan.
Apr.
Jul.
NOv.
1988
Time in days

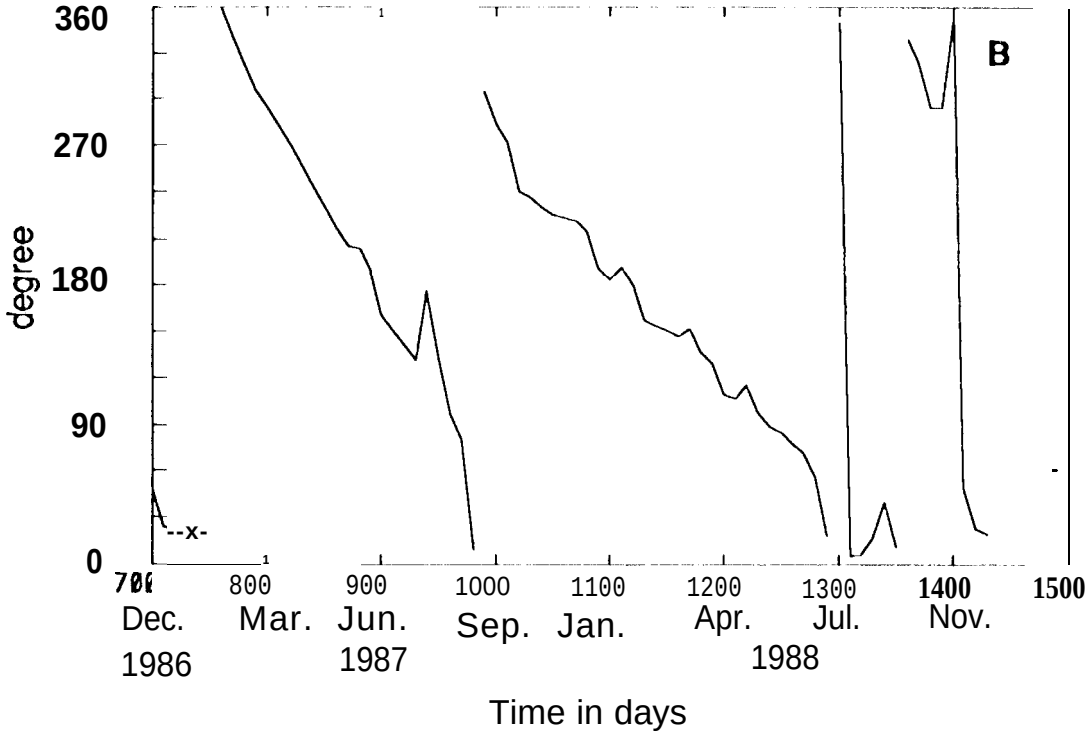
360
270
180
90
0
degree
B
--x-
700
800
900
1000
1100
1200
1300
1400
1500
Dec.
1986
Mar.
Jun.
1987
Sep.
Jan.
Apr.
Jul.
Nov.
1988
Time in days

Figure 6

A

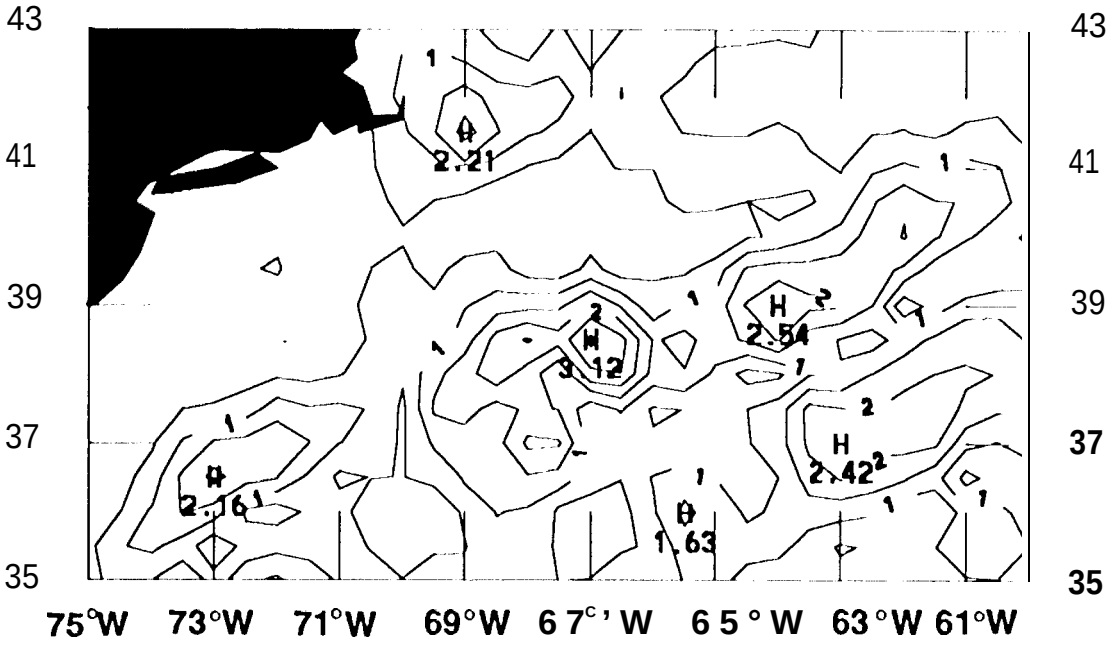
43
41
39
37
35
H
2.21
H
2.54
H
3.12
H
2.42
H
2.16
H
1.63
75°W 73°W 71°W 69°W 67°W 65°W 63°W 61°W

B

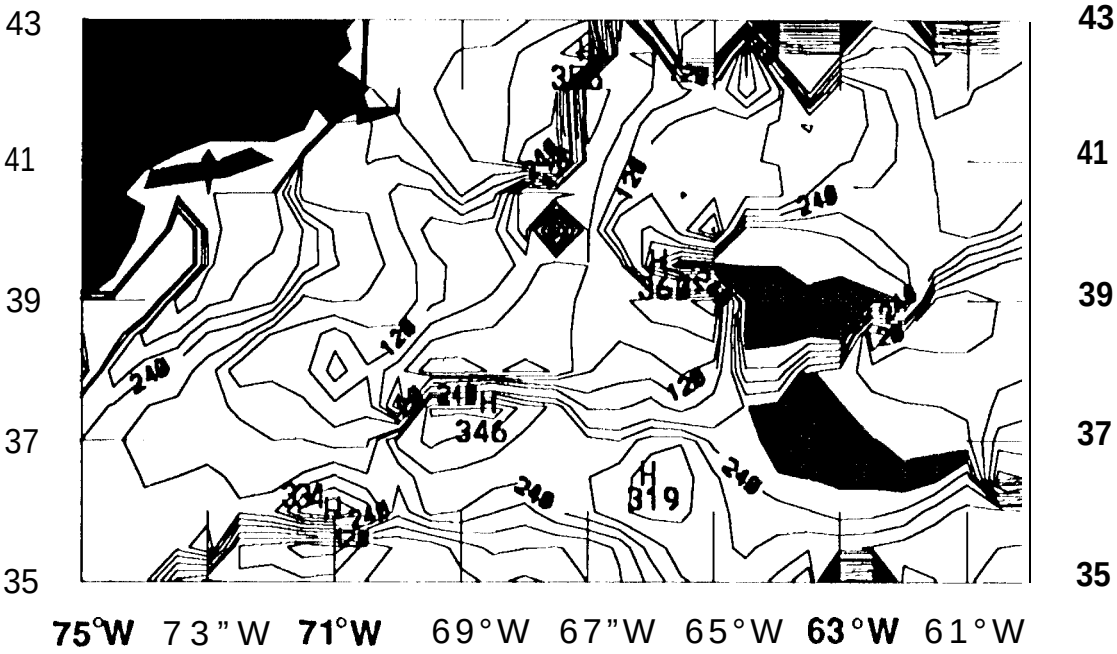
43
41
39
37
35
H
346
H
319
75°W 73°W 71°W 69°W 67°W 65°W 63°W 61°W

Figure 7

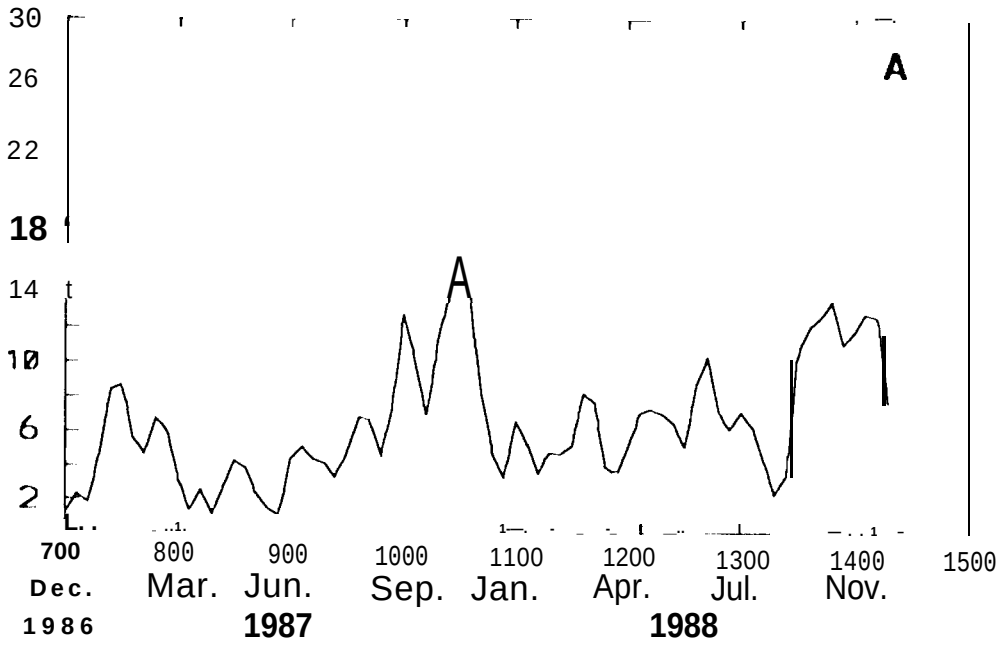

Time in days

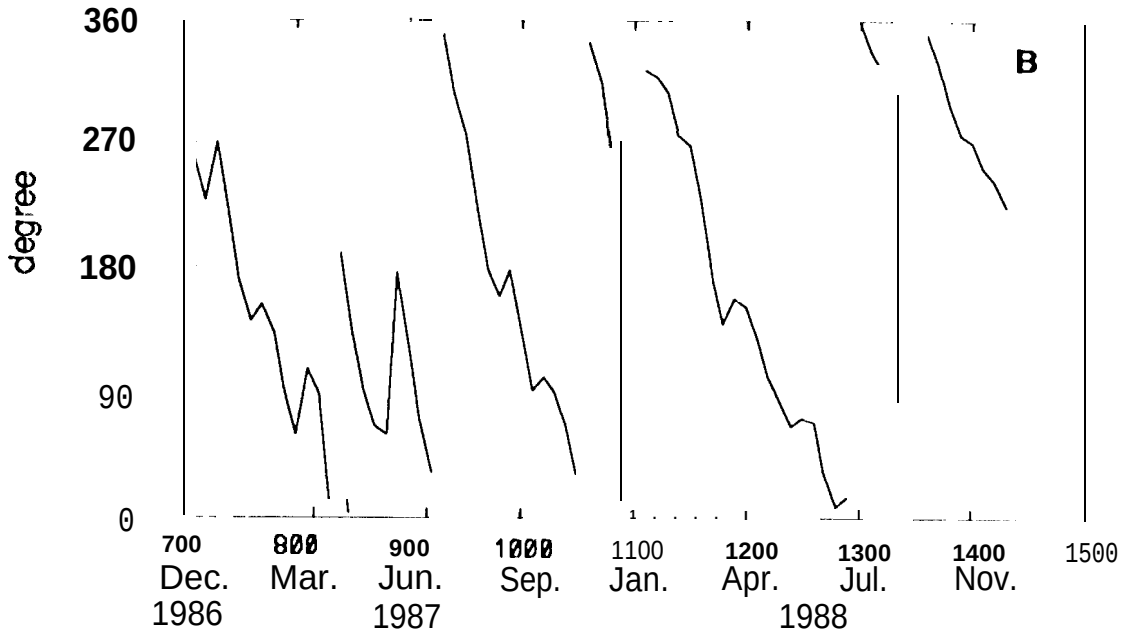

Time in days

Figure 8

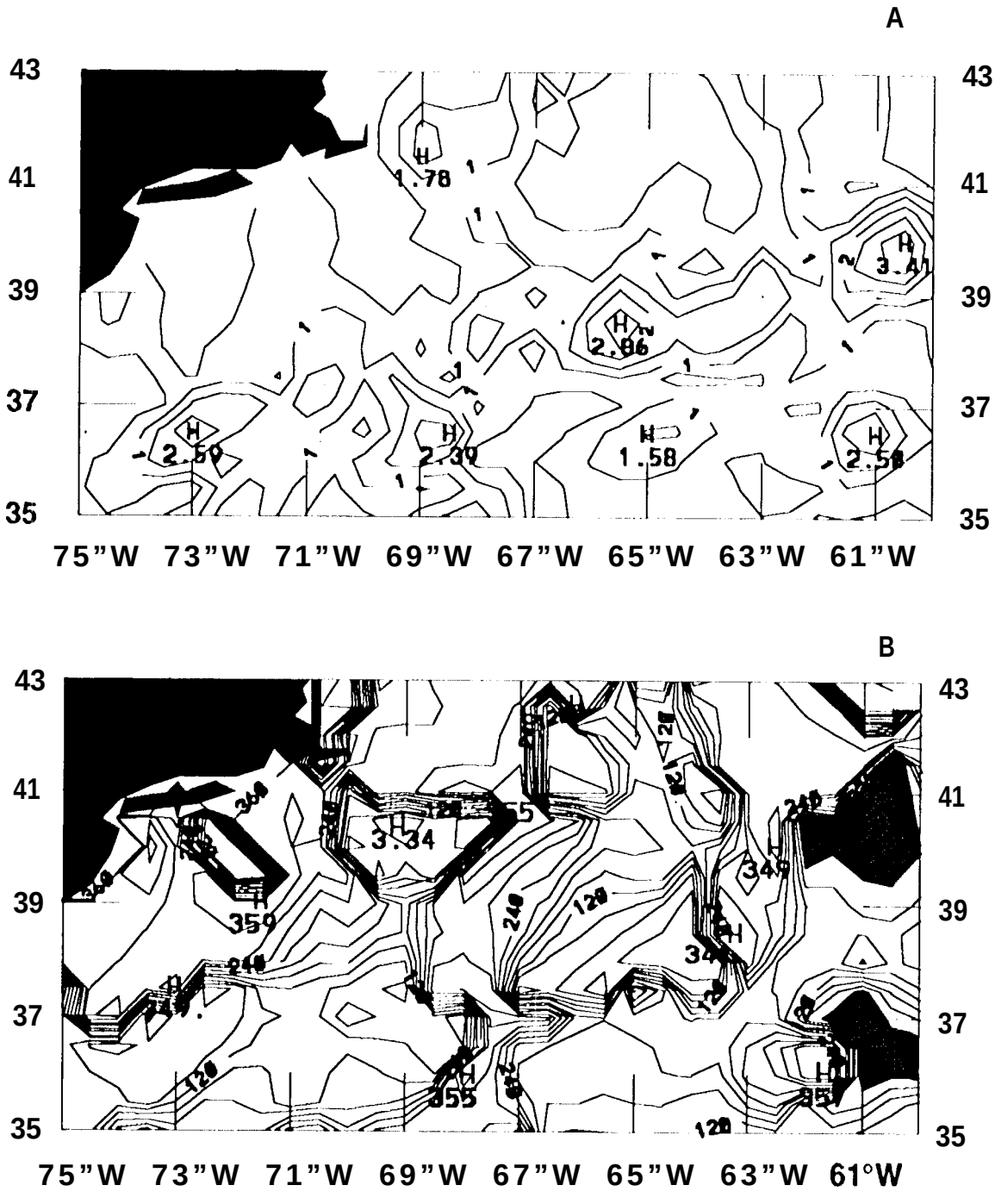
A
43
41
39
37
35
H
1.78
H
3.41
H
2.86
H
2.59
H
2.39
H
1.58
H
2.56
75"W 73"W 71"W 69"W 67"W 65"W 63"W 61"W
B
43
41
39
37
35
H
3.34
H
359
H
355
75"W 73"W 71"W 69"W 67"W 65"W 63"W 61°W

Figure 9

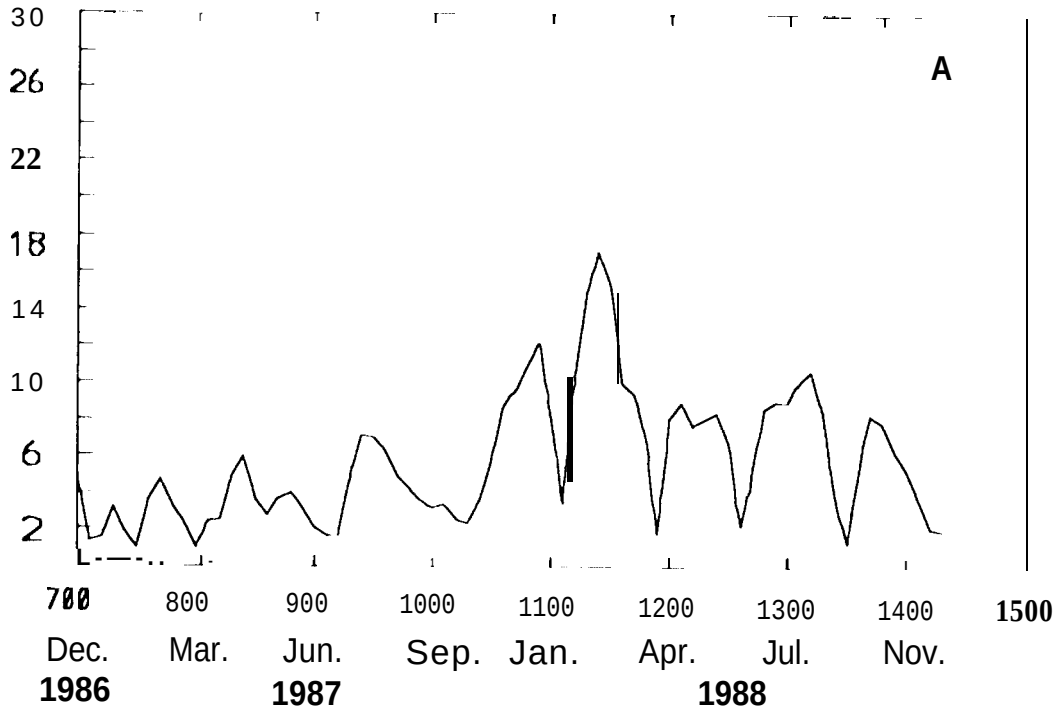

Time in days

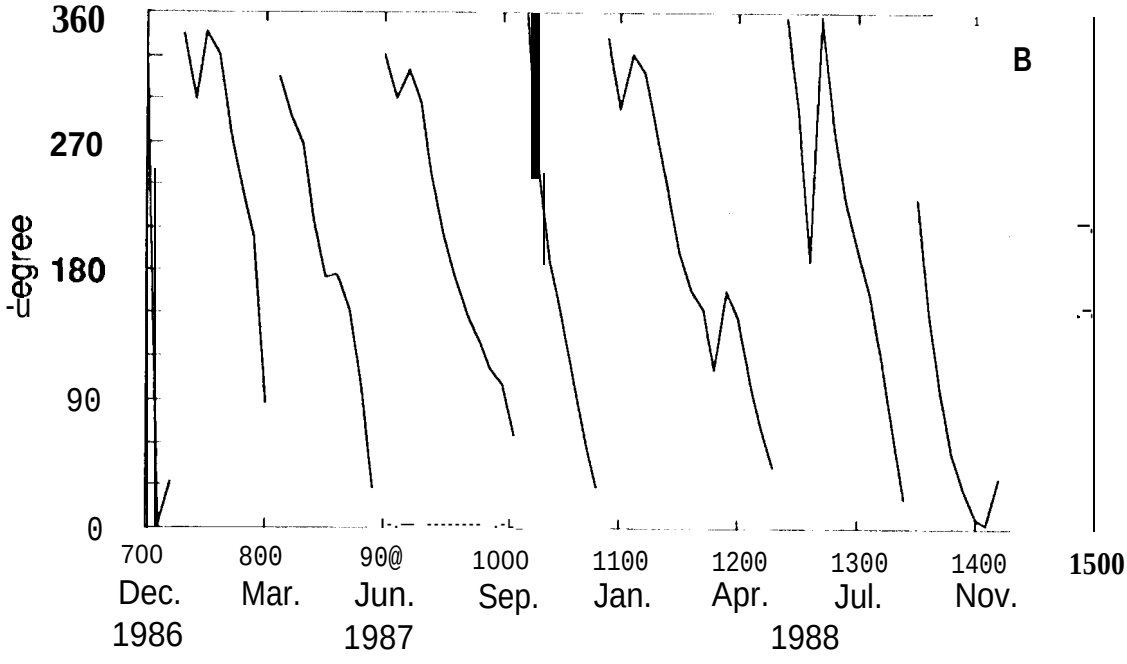

Time in days

Figure 10

A

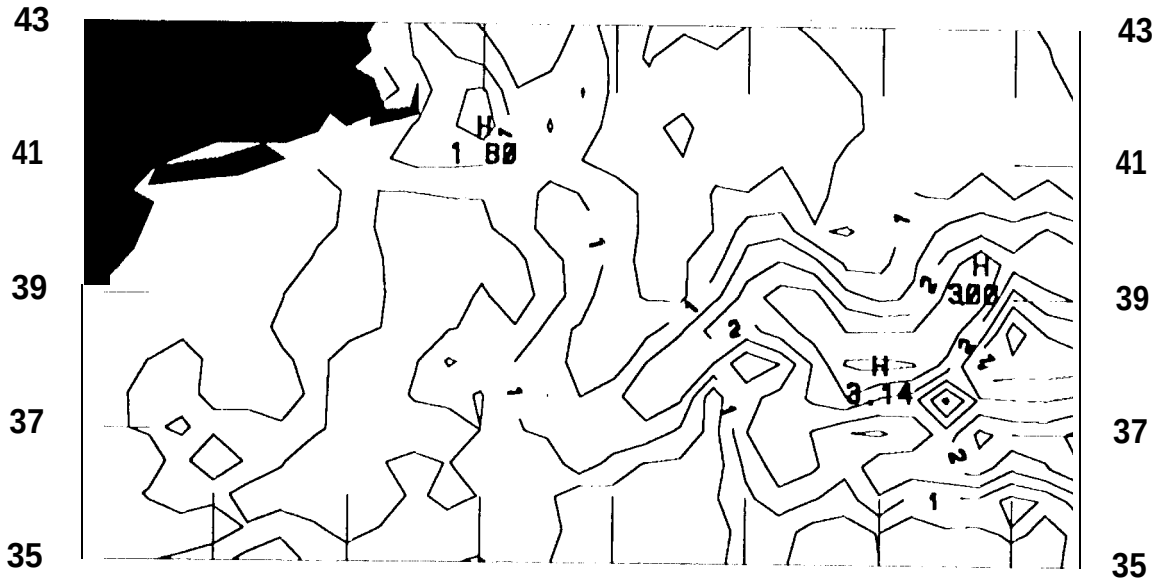

75"W 73"W 71°W 69°W 67"W 65"W 63"W 61"W

B

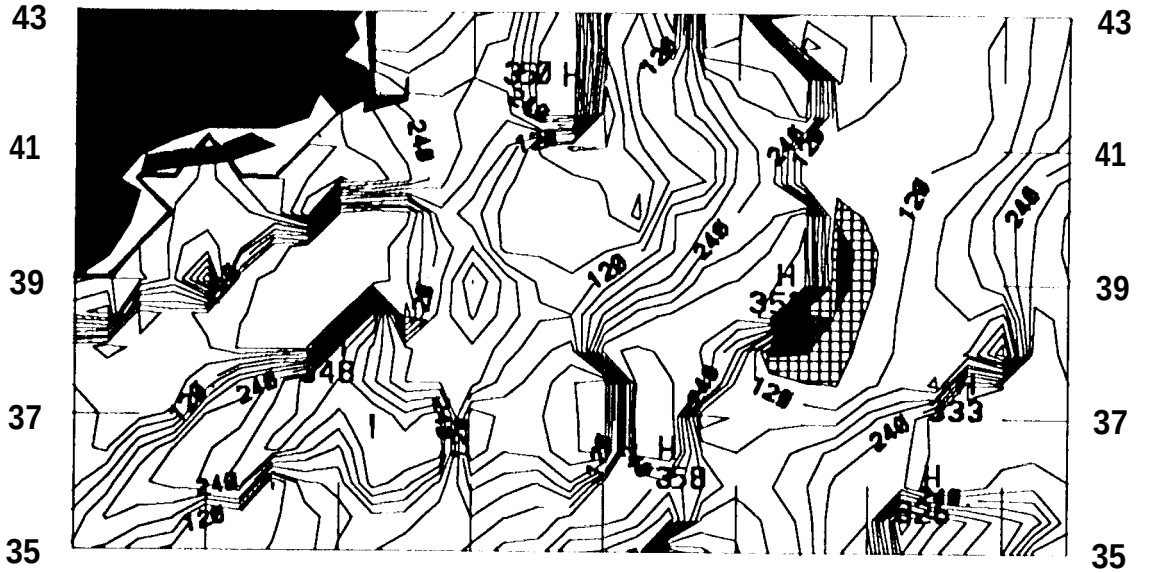

75°W 73"W 71°W 69" W 67"W 65"W 63°W 61°W

Figure 11

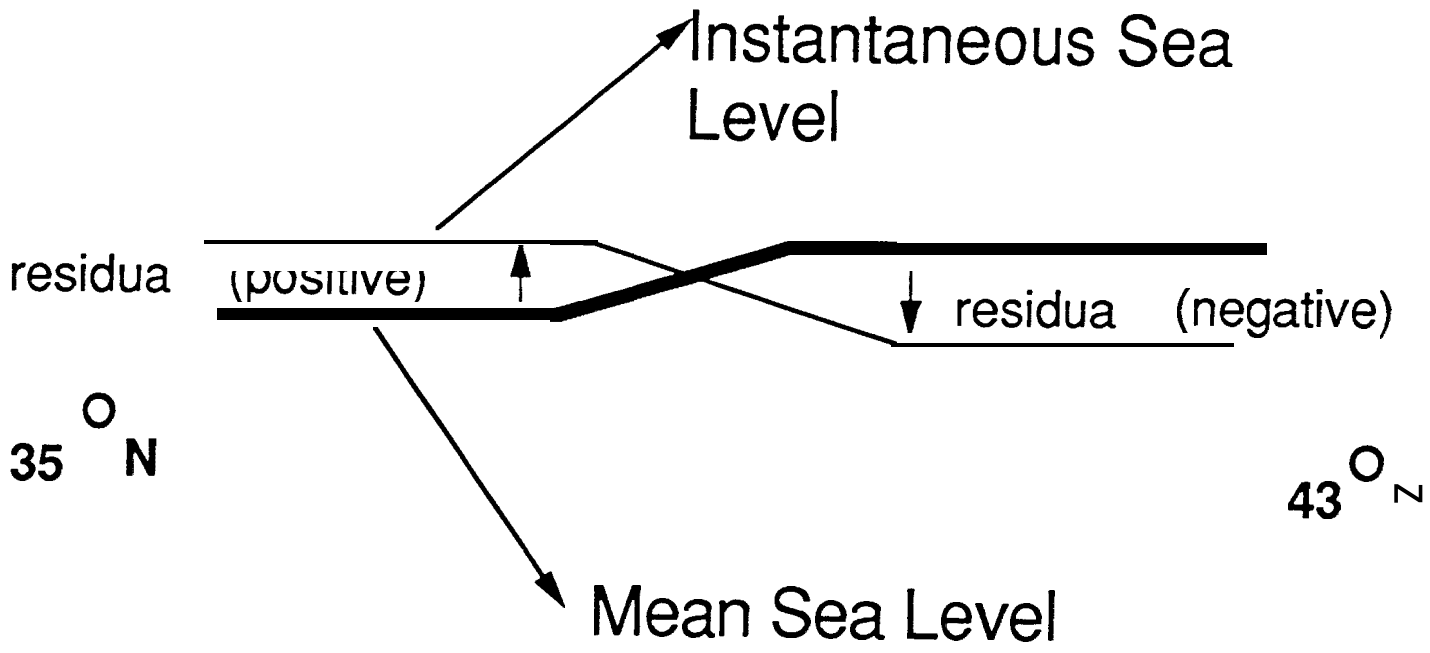
Instantaneous Sea Level
residua (positive)
residua (negative)
35 O N
43 O N
Mean Sea Level

Figure 12

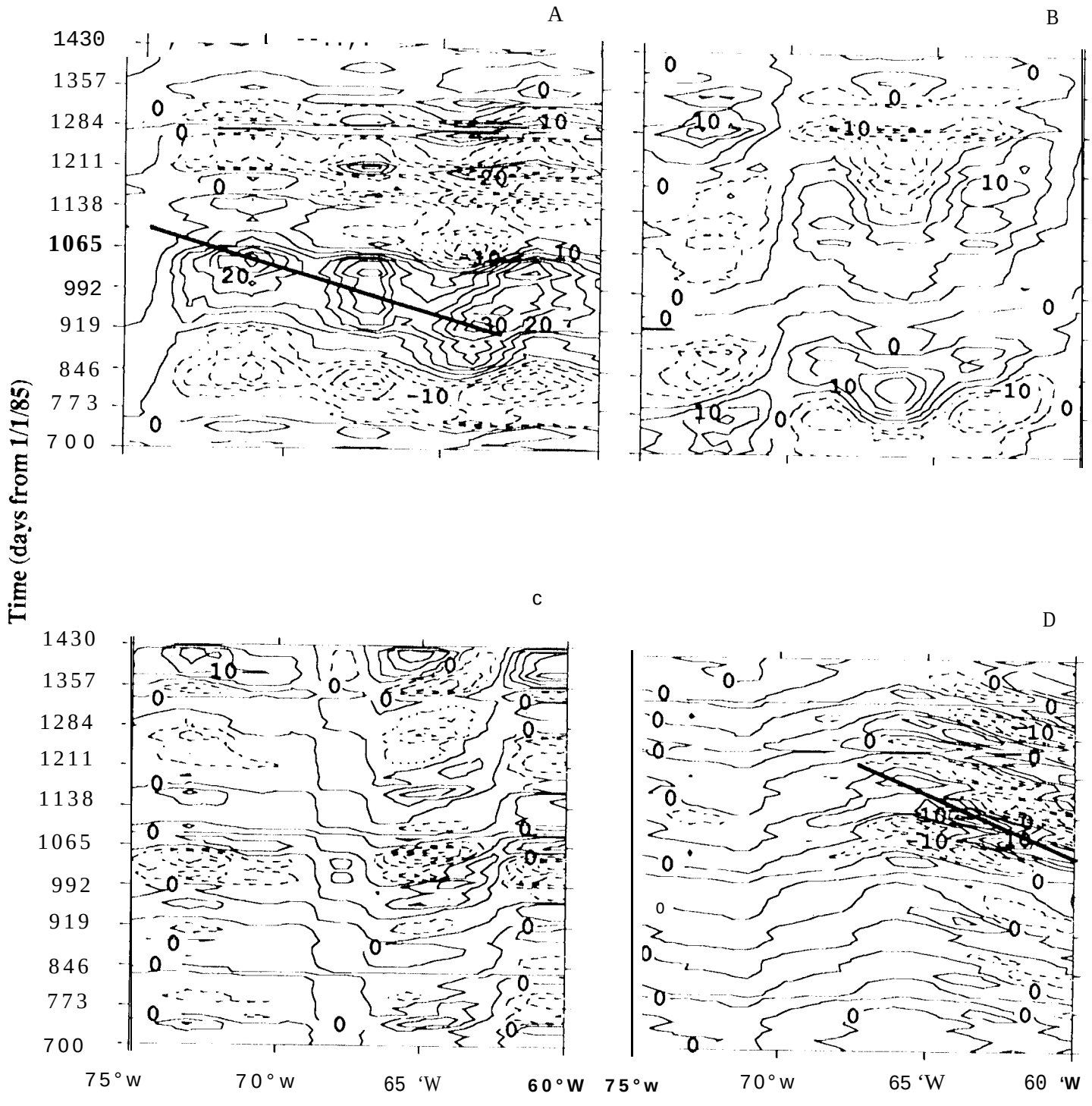
A
B
C
D
1430
1357
1284
1211
1138
1065
992
919
846
773
700
Time (days from 1/1/85)
75°w
70°w
65 'W
60°W
75°w
70°w
65 'W
60 'W
Longitude

Figure 13

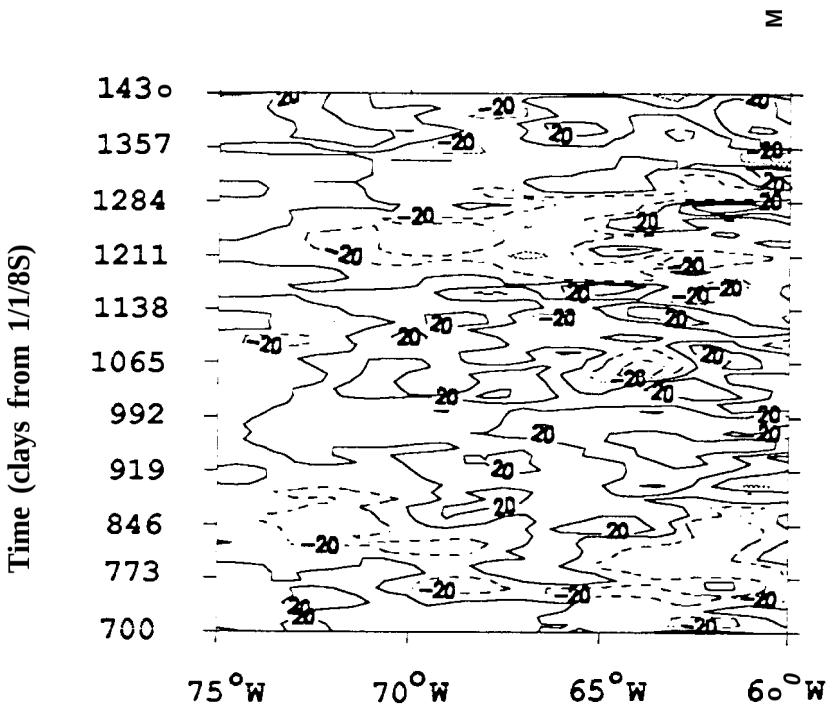
Time (clays from 1/1/8S)
143o
1357
1284
1211
1138
1065
992
919
846
773
700
75°W
70°W
65°W
6o°W

Figure 13

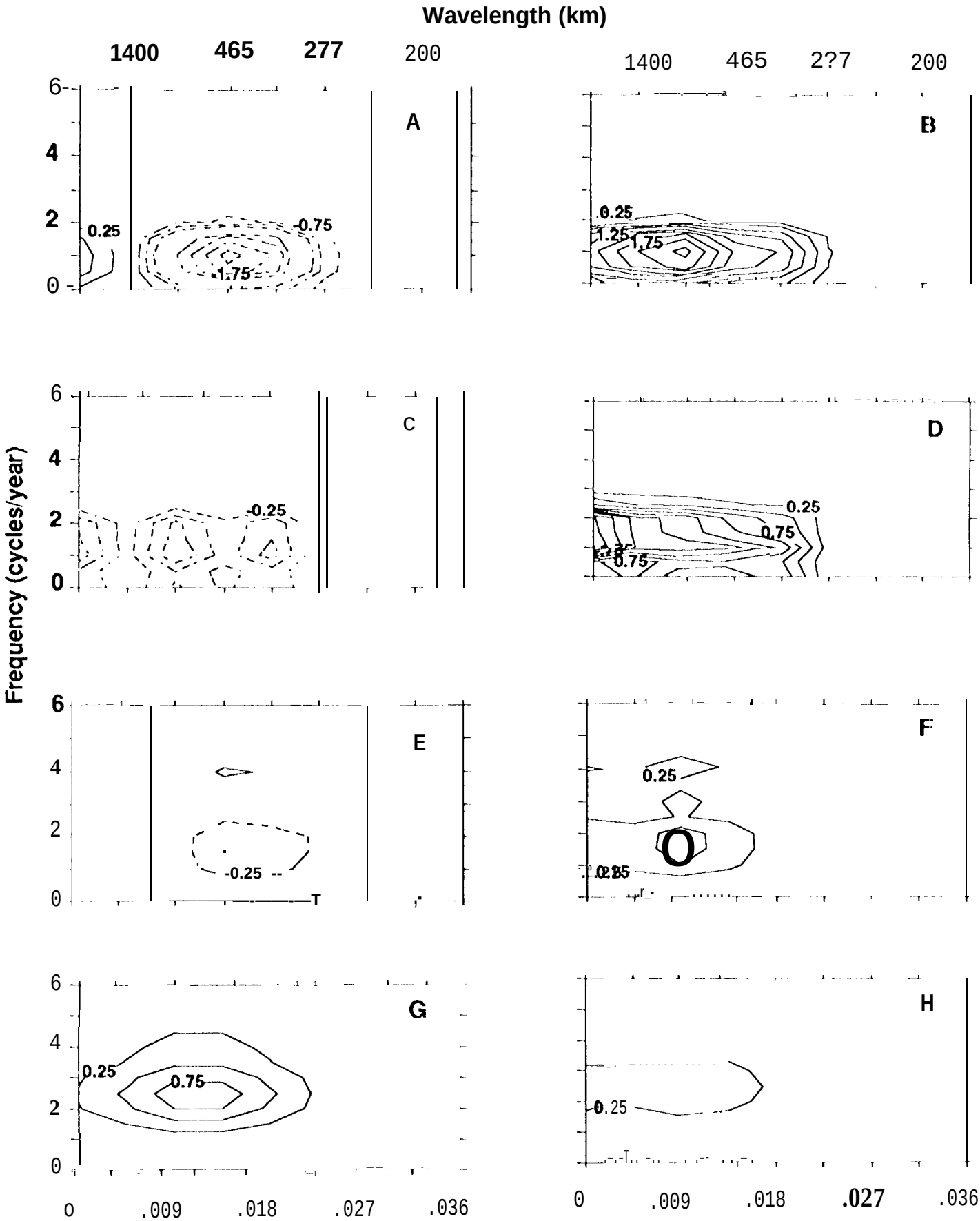
Wavelength (km)
1400
465
277
200
A
B
C
D
E
F
G
H
0.25
0.75
1.25
1.75
-0.25
-0.75
Frequency (cycles/year)
0
2
4
6
0
.009
.018
.027
.036
Wavenumber (radians/km)

Figure 14

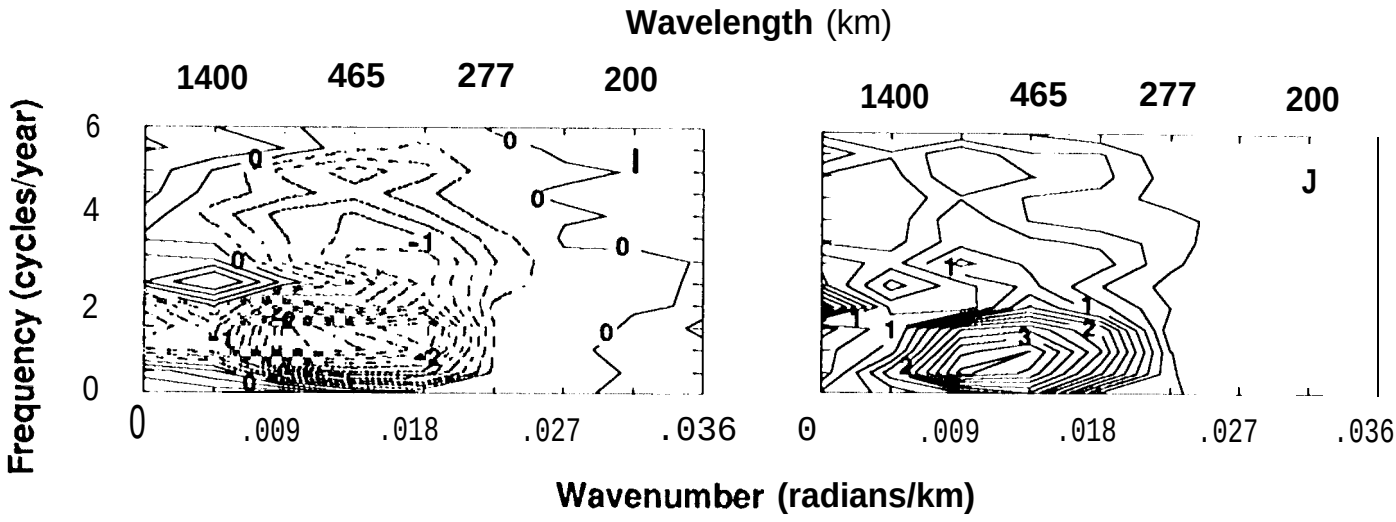
Wavelength (km)
1400
465
277
200
1400
465
277
200
Frequency (cycles/year)
6
4
2
0
I
J
0
.009
.018
.027
.036
0
.009
.018
.027
.036
Wavenumber (radians/km)

Figure 14

A

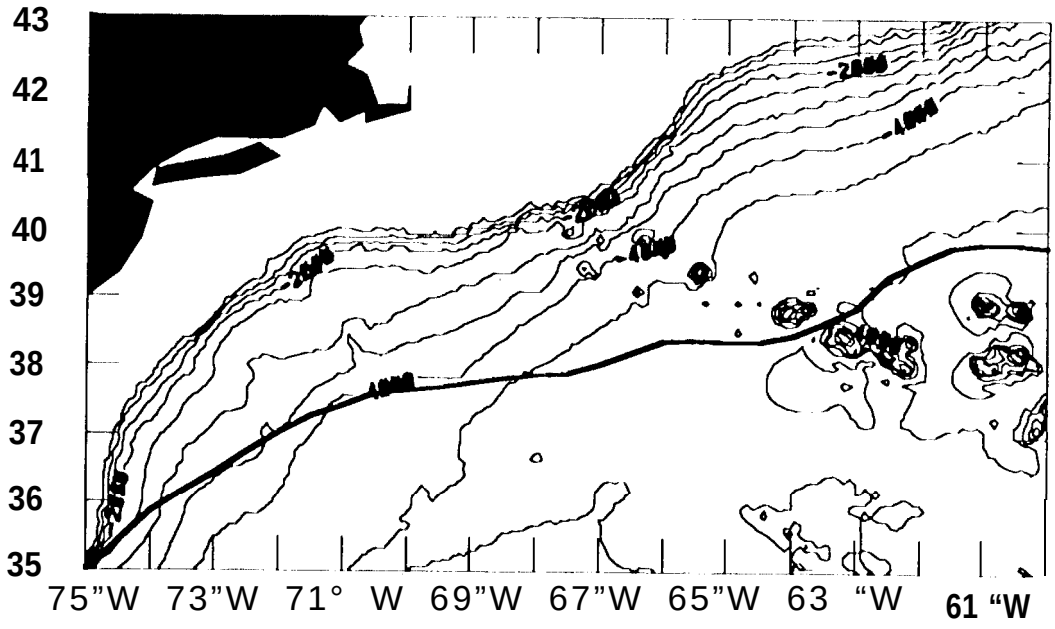
43
42
41
40
39
38
37
36
35
75"W 73"W 71° W 69"W 67"W 65"W 63 "W
61 "W

B

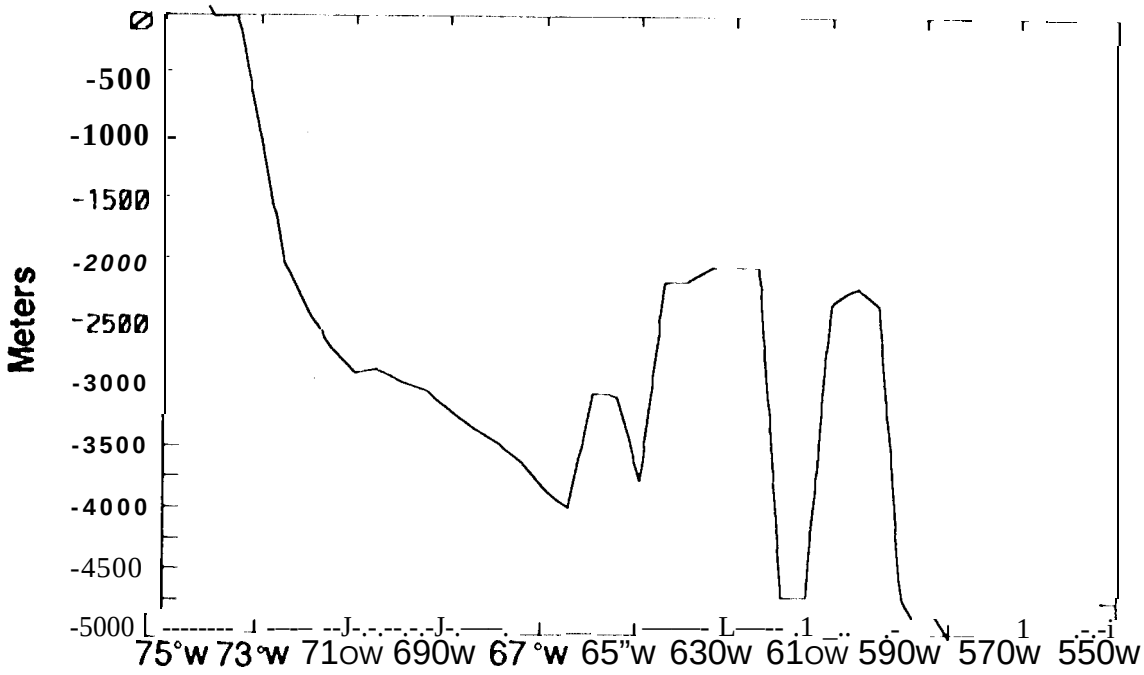
Meters
0
-500
-1000
-1500
-2000
-2500
-3000
-3500
-4000
-4500
-5000
75°w 73°w 71ow 690w 67°w 65"w 630w 61ow 590w 570w 550w
Longitude

Figure 15